

Electronic Supplementary Information

**Hexaphenylbenzene based AIEE active probe for the
preparation of ferromagnetic α -Fe₂O₃ nanoparticles:
Facile Synthesis and catalytic applications**

Subhamay Pramanik, Vandana Bhalla* and Manoj Kumar*

*Department of Chemistry, UGC Sponsored Centre for Advanced Studies-1, Guru Nanak Dev
University, Amritsar 143005, and Punjab, India*

vanmanan@yahoo.co.in, mksharmaa@yahoo.co.in

- S4-S5** General Experimental Procedures.
- S6** Synthesis of α -Fe₂O₃ nanoparticles and catalysis in photo degradation the aqueous solution Rhodamine B (RhB) dye and C-C Sonogashira-Hagihara coupling reactions.
- S7** Synthetic route and characteristic data of compound **3**.
- S8-S9** Comparison of present synthesis method over other reported procedure in literature for the preparation of ferromagnetic α -Fe₂O₃ nanoparticles.
- S10** Comparison of present probe **3** for Fe³⁺ ions detection over other reported chemosensors for Fe³⁺ ion reported in the literature.
- S11** Comparison of present method over other reported procedure in literature for the C-C Sonogashira coupling reactions by α -Fe₂O₃/other iron oxide nanoparticles prepared by derivative **3**.
- S12** Comparison of present method over other reported procedure in literature for photocatalytic degradation Rhodamine B (RhB) dye by ferromagnetic α -Fe₂O₃ nanoparticles prepared by derivative **3**.
- S13** Comparison of catalytic activity α -Fe₂O₃ nanoparticles for the Sonogashira coupling reactions over other noble metal catalysts like Pd, Au, Ag, Ru etc. reported in the literature.
- S14** UV-vis and fluorescence spectra of **3** in the presence of in different percentage of water in ethanol.

- S15** Fluorescence spectra of **3** at different concentration in Ethanol.
- S16** Fluorescence spectra of **3** in the presence of in different percentage TEG in Ethanol and Variation in quantum yield value with the variation of water fractions in ethanol solution of derivative **3**.
- S17** Time resolved fluorescence decays of **3** with increasing water fraction upto 70% and the table showing the radiative, non-radiative decay rate constants.
- S18** Concentration dependent ^1H NMR spectra of compound **3** in DMSO- d_6 .
- S19** Graphical representation of rate constant of formation of $\alpha\text{-Fe}_2\text{O}_3$ nanoparticles.
- S20** UV-vis spectra of compound **3** upon additions of various metal ions as their perchlorate and chloride salt in $\text{H}_2\text{O}/\text{EtOH}$ (7:3, v/v).
- S21** UV-vis spectral changes of **3** on addition of Fe^{3+} ions at different pH; the effect of pH on the UV-vis spectrum of **3**.
- S22** Plot of fluorescence quenching efficiency of the ratiometric probe **3** as a function of the Fe^{3+} ions concentration.
- S23** Detection limit of Fe^{3+} by using compound **3** in $\text{H}_2\text{O}/\text{EtOH}$ (7:3, v/v).
- S24** Competitive and selectivity graph of derivative **3** towards various metal ions as their perchlorate and chloride salt in $\text{H}_2\text{O}/\text{EtOH}$ (7:3, v/v).
- S25** Time resolved fluorescence decays of **3** in $\text{H}_2\text{O}/\text{EtOH}$ (7:3, v/v) mixture on addition of Fe^{3+} ions.
- S26** Photographs of fluorescence response of derivative **3** coated fluorescent paper strip in presence of aqueous solution of Fe^{3+} .
- S27** Overlay ^1H NMR spectra of **3** and $\alpha\text{-Fe}_2\text{O}_3$ nanoparticles of **3** after filtration with THF.
- S28** Photographs of SEM images of aggregates of **3** in presence of Fe^{3+} ions. TEM images of $\alpha\text{-Fe}_2\text{O}_3$ nanoparticles and size distribution bar diagram.
- S29** EDX spectra and XRD pattern of $\alpha\text{-Fe}_2\text{O}_3$ -nanoparticles.
- S30** Dynamic light scattering (DLS) results showing the particle size diameter of the aggregates of **3** in $\text{H}_2\text{O}/\text{EtOH}$ (7:3, v/v) mixture and $\alpha\text{-Fe}_2\text{O}_3$ nanoparticles.

- S31** FT-IR spectrum of α -Fe₂O₃ nanoparticles.
- S32** The magnetic hysteresis loop of α -Fe₂O₃ nanorods at room temperature.
- S33** UV-vis spectrum showing the photo catalytic degradation of RhB solutions (0.1 mM) in the presence of α -Fe₂O₃ nanoparticle (2 μ M) with 2 mM H₂O₂ and the rate constant of photo catalytic degradation of RhB dye by α -Fe₂O₃ nanoparticles.
- S34** Catalytic application of α -Fe₂O₃ nanoparticles in palladium, CuI and amine free Sonogashira cross coupling reactions.
- S35-S36** Comparison of catalytic activity α -Fe₂O₃ nanoparticles for the mentioned Sonogashira coupling reactions over other reported procedure in literature.
- S37** ¹H and ¹³C NMR of spectrum of 5a.
- S38** ESI-MS spectrum of 5a.
- S39** ¹H and ¹³C NMR of spectrum of 5b.
- S40** ESI-MS spectrum of 5b.
- S41** ¹H NMR of spectrum of derivative **3**.
- S42** ¹³C NMR of spectrum of derivative **3**.
- S43** ESI-MS spectrum of derivative **3**.
- S44** FT-IR spectrum of compound **3**.

General Experimental Procedures:

Materials and reagents: All reagents were purchased from Aldrich and were used without further purification. THF was dried over sodium and benzophenone as an indicator. UV-vis studies were performed in THF, absolute ethanol, distilled water and HEPES buffer (0.05 M) (pH = 7.05).

Instrumentation: UV-vis spectra were recorded on a SHIMADZU UV-2450 spectrophotometer, with a quartz cuvette (path length, 1 cm). The cell holder was thermostatted at 25°C. The fluorescence spectra were recorded with a SHIMADZU-5301 PC spectrofluorimeter. UV-vis spectra were recorded on Shimadzu UV-2450PC spectrophotometer with a quartz cuvette (path length: 1 cm). The cell holder was thermostatted at 25 °C. The scanning electron microscope (SEM) images were obtained with a field-emission scanning electron microscope (SEM CARL ZEISS SUPRA 55). The TEM mages was recorded from Transmission Electron Microscope (TEM) - JEOL 2100F. The FT-IR spectra were recorded with VARIAN 660 IR Spectrometer. The dynamic light scattering (DLS) data were recorded with MALVERN Instruments (Nano-ZS). The Time resolved fluorescence spectra were recorded with a HORIBA Time Resolved Fluorescence Spectrometer. Elemental analysis was done using a Flash EA 1112 CHNS/O analyzer from Thermo Electron Corporation. ¹H and ¹³C NMR spectra were recorded on a BRUKER-AVANCE-II FT-NMR-AL400 MHz and 500 MHz spectrophotometer using CDCl₃, DMSO-d₆, D₂O as solvent and tetramethylsilane, SiMe₄ as internal standards. Data are reported as follows: chemical shifts in ppm (1), multiplicity (s = singlet, br = broad signal, d = doublet, t = triplet, m = multiplet), coupling constants *J* (Hz), integration and interpretation. Silica gel 60 (60–120 mesh) was used for column chromatography.

Quantum yield calculations: Fluorescence quantum yield was determined by using optically matching solution of diphenylanthracene ($\Phi_{fr} = 0.90$ in cyclohexane) as standard at an excitation wavelength of 373 nm and quantum yield is calculated using the equation:

$$\Phi_{fs} = \Phi_{fr} \times \frac{1-10^{-A_r L_r}}{1-10^{-A_s L_s}} \times \frac{N_s^2}{N_r^2} \times \frac{D_s}{D_r}$$

Φ_{fs} and Φ_{fr} are the radiative quantum yields of sample and the reference respectively, A_s and A_r are the absorbance of the sample and the reference respectively, D_s and D_r the respective areas of emission for sample and reference. L_s and L_r are the lengths of the absorption cells of sample and reference respectively. N_s and N_r are the refractive indices of the sample and reference solutions (pure solvents were assumed respectively).

UV-vis and fluorescence titrations: The concentration of HEPES buffer (pH = 7.05) is 0.05 M. For each experiment we have taken 3 ml solution which contains solution of derivative **3** in 15 μ l of THF diluted with 885 μ l of EtOH and 2.1 ml HEPES buffer (0.05 M, pH = 7.05) or double distilled water. UV-vis and fluorescence titrations were performed with 5.0 μ M solutions of ligand (15 μ l of THF are used to dissolve) in H₂O/EtOH (7:3, v/v). Typically, aliquots of freshly prepared standard solutions (10^{-1} M to 10^{-3} M) of metal ions such as Zn²⁺, Hg²⁺, Cu²⁺, Fe²⁺, Fe³⁺, Co²⁺, Pb²⁺, Ni²⁺, Cd²⁺, Ag⁺, Ba²⁺, Al³⁺, Mg²⁺, K⁺ and Na⁺ ions as their perchlorate [M(ClO₄)_x; X = 1-3]/chloride [M(Cl)_x; X = 1-3] in EtOH were added to record the UV-vis and fluorescence spectra.

Synthesis of α -Fe₂O₃ Nanoparticles:

Aqueous solution of 0.1 M FeCl₃ (150 μ L) was added to a 3 ml solution of compound **3** (0.2 mM) in H₂O/EtOH (7:3, v/v). The reaction was stirred at room temperature for 30 min and formations of nanoparticles take place. These nanoparticles solution was used as such in the catalytic experiment.

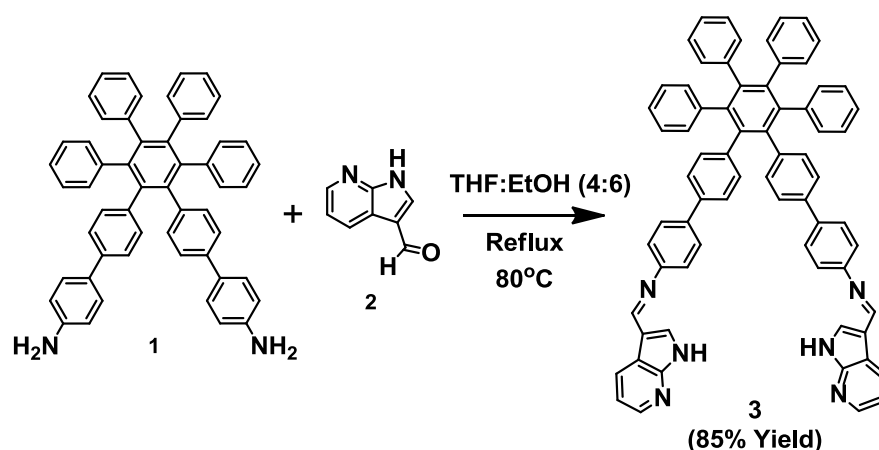
Measurement of photo catalytic degradation Rhodamine B (RhB) dye by α -Fe₂O₃ Nanoparticles:

The photocatalytic activity of the as-prepared samples was evaluated by photocatalytic degradation of RhB pollutants at room temperature. The experimental procedures were performed as follows. 3 mL of 5×10^{-5} M RhB aqueous solution, 30 μ L of 2 mM H₂O₂ and 5 μ L (2 μ M) of α -Fe₂O₃ nanoparticles of derivative **3** were mixed. After stirring the reaction mixture for 26 min, fully colour change of the reaction mixture from pink to colourless was observed which indicate the degradation Rhodamine B.

C-C cross coupling via the Sonogashira-Hagihara reaction by α -Fe₂O₃ Nanoparticles:

Here, we use α -Fe₂O₃ Nanoparticles (<20 nm) as an efficient catalyst for carbon-carbon bond formation via the Sonogashira-Hagihara reaction under palladium, copper and amine-free conditions using ethylene glycol (EG) as a solvent and K₂CO₃ as a base. The effect of different solvents upon the reaction of aryl-iodide (**4a-b**, 1 mmol) with phenylacetylene (100 mg, 1 mmol) as a model reaction in the presence of K₂CO₃ (276 mg, 2 mmol) and 5 mol% of the Nano catalyst (α -Fe₂O₃) at 80°C was studied (Table 1). The results show that ethylene glycol (EG) is a suitable solvent for the reaction. EG possesses negligible vapour pressure, is thermally stable, and is not so expensive with a low toxicity. Ethylene glycol is highly soluble in water, and can be easily separated from the organic phase by addition of water to the reaction mixture. The products (**5a-b**) are purified by Silica gel 60 (60-120 mesh) and the isolated yield has been given.

Synthetic scheme of compound 3:



Scheme 1. Synthesis of hexaphenylbenzene based derivative **3**.

Synthesis of compound 3:

A clear solution of compound **1** (0.05 g, 0.07 mmol) and **2**, 7-azaindole-3-carboxaldehyde **2** (0.023 g, 0.15 mmol) in dry THF:MeOH (4:6) was stirred at 80°C. After 24 h, the reaction mixture turned turbid. The reaction mixture was concentrated under the reduced pressure and dry methanol was poured into it, solid appears. The solid was filtered and recrystallized from methanol to afford the light yellow coloured compound **3** (0.058 g, 85%); mp: >280°C (Scheme 1). The structure of compound **3** was confirmed from its spectroscopic and analytical data (Fig. S26-S29, ESI†). ¹H NMR (400 MHz, DMSO-d₆, ppm) δ = 12.36 (s, 2H, -NH), 9.46 (s, 2H, -HC=N), 8.74 (s, 2H, ArH), 8.69 (d, *J* = 8 Hz, 2H, ArH), 8.54 (s, 2H, ArH), 8.48-8.38 (m, 4H, ArH), 8.19 (s, 2H, ArH), 7.58 (s, 2H, ArH), 7.34 (d, *J* = 8 Hz, 2H, ArH), 7.26 (d, *J* = 8 Hz, 4H, ArH), 7.15 (t, *J* = 8 Hz, 8H, ArH), 7.06 (d, *J* = 8 Hz, 4H, ArH), 6.95-6.91 (m, 10H, ArH), 6.56 (d, *J* = 8 Hz, 2H, ArH). ¹³C NMR (100 MHz, DMSO-d₆, ppm) δ = 161.10, 156.26, 150.55, 145.89, 143.82, 140.21, 139.94, 139.69, 135.77, 135.12, 131.42, 131.08, 130.81, 127.15, 126.26, 126.16, 124.80, 123.95, 117.37, 116.22, 114.88. ESI-MS mass spectrum of compound **3** showed a parent ion peak, *m/z* = 973.3970 [M+H]⁺ and fragmentation peaks *m/z* = 845.3595 [A+H]⁺ and *m/z* = 717.3265 [B+H]⁺. The FT-IR spectrum of compound **3** showed stretching band at 1621 cm⁻¹ corresponding to -HC=N group and 3382 cm⁻¹ corresponds to -NH group. Elemental analysis: Calculated for C₇₀H₄₈N₆: C 86.39; H 4.97; N 8.64; Found: C 86.38%; H 4.97%; N 8.63%.

Table S1: Comparison of this method in present manuscript over other reported procedure in literature for the preparation of α -Fe₂O₃ nanoparticles.

S. No.	Publication	Method of formation of α -Fe ₂ O ₃ nanoparticles	Reagent Used	Reducing/Oxidising agent Used	Reaction time to prepare α -Fe ₂ O ₃ nanoparticles	Temp. (°C)	Size	Shape of α -Fe ₂ O ₃ nanoparticles	Recyclability by magnet after reaction
1	Present manuscript	Wet Chemical Method	Compound 3 in Water/EtOH and FeCl ₃	No	30 min	Room Temperature	10-15 nm (length)	Nanorods	Yes
2	<i>Chem. Commun.</i> , 2014, 50 , 8036	Microwave followed by heating and reduction	Graphite-Fe(CO) ₅	Yes (5% H ₂ /Ar)	20 sec followed by 2 h heating	600	0.4-0.6 μ m	Submicron-wires 0.4-0.6 μ m (average: 0.49 μ m)	Yes
3	<i>J. Mater. Chem. A</i> , 2014, 2 , 10662	Sequential pulsing of TBF in O ₂ plasma and atomic layer deposition	Tertiary butyl ferrocene (TBF) and O ₂ plasma in He and 5% H ₂ /He	Yes (O ₂ plasma)	50 min	150-350	16-45 nm	film	No
4	<i>Chem. Commun.</i> , 2014, 50 , 1215	Hydrothermal method and nanocasting technique	Fe(NO ₃) ₃ ·9H ₂ O and Graphite (GNS)	No	24h/10h	40/200	2 nm	Nanocrystals	No
5	<i>Energy Environ. Sci.</i> , 2014, 7 , 451	Bacterial iron biomineralization and annealing	<i>Acidovorax</i> sp. Strain of BoFeN1/g-FeOOH under N ₂ /H ₂ (95/5) atmosphere (p(O ₂) < 5 Pa)	Yes (Bacteria)	1 h	700	48±18 nm	Hollow bacteriomorphs	No
6	<i>Chem. Mater.</i> , 2014, 26 , 2105	Reduction and hydrothermal	TEOS, PLL, CTAB, Gd-DTPA, FeCl ₃ , NaCl and KH ₂ PO ₄	Yes (KH ₂ PO ₄)	72 h	100	420 ± 20 nm	Spindle shaped	Yes
7	<i>ACS Catal.</i> , 2014, 4 , 990	Ammonia-modified hydrothermal process and wet-chemical method	FeCl ₂ , HCl, N ₂ atm.	No	8 h	1100 (Inert atm.)	~16 nm	Spherical	No
8	<i>ACS Appl. Mater. Interfaces</i> , 2014, 6 , 1113	Hydrothermal	FeCl ₃ ·6H ₂ O, Na ₂ HPO ₄ ·12H ₂ O, Water, EtOH	Yes	14 h	105	240 nm	Spindle	Yes
9	<i>ACS Appl. Mater. Interfaces</i> , 2014, 6 , 7189	Chemical vapor deposition	FeCl ₃ , Water, EtOH, Nanomesh graphene (NMG)	Yes (NH ₃ ·H ₂ O, 25 wt %)	1 h	450	100 nm	Spindle	No
10	<i>Inorg. Chem.</i> , 2014, 53 , 2304	Thermal Decomposition Approach	Iron acetate [Fe(ac) ₂], trioctylphosphine oxide, hexadecylamine, 1-octadecene	No	5 h	400	12-45 nm	Mesoporous structure	No
11	<i>Cryst. Eng. Comm.</i> , 2014, 16 , 1451	Hydrothermal growth	FeCl ₃ , NaH ₂ PO ₄ . Solutions	Yes	7 days	100	≤ 5 nm	Spindles	No

12	<i>Cryst. Eng. Comm.</i> , 2014, 16 , 5566	Hydrothermal process	Iron(III) nitrate with zinc and cupric ions additives	Yes	16 h	160	300 nm	Quasi-thorhombic	No
13	<i>Cryst. Growth Des.</i> , 2014, 14 , 1039	Solvothermal process	Fe(NO ₃) ₃ ·9H ₂ O, Sucrose solution, SBA-15	No	3 days	1100	40 nm	Nanorods	No
14	<i>Cryst. Eng. Comm.</i> , 2014, 16 , 1553	Solvothermal method by controlled hydrolysis	Fe(acac) ₃ in ethanol and water	No	24 h	150	20 nm	Disc-like nanostructures	No
15	<i>Phys. Chem. Chem. Phys.</i> , 2014, 16 , 4284	Electrodeposition (anodization method) followed by annealing	FeCl ₂ solution (pH = 4.1, adjusted by 1 M HCl), EG, Water	No	2 h	500	20-150 nm	Nanotubular	No
16	<i>Chem. Commun.</i> , 2013, 49 , 8695	Spray drying method followed by annealing	Fe(NO ₃) ₃ ·9H ₂ O (10 mmol) and sucrose (10 mmol), N ₂ atm.	No	5 h	400	30-3000 nm	Multishelled hollow spheres	No
17	<i>Green Chem.</i> , 2013, 15 , 3077	Hydrolysis reaction, coprecipitation and dehydration	FeCl ₂ ·4H ₂ O and [Fe(NO ₃) ₃ ·9H ₂ O inert atmosphere	Yes	2 h	90	8-10 nm	Cubic	Yes
18	<i>Chem. Mater.</i> , 2013, 25 , 1549	Molten salt syntheses (pyrolysis)	FeCl ₃ ·6H ₂ O, HCl, heat	No	24 h	100	425 ± 119	Hexagonal nanoplates	No
19	<i>J. Phys. Chem. C</i> , 2013, 117 , 11242	Hydrothermal method	FeCl ₃ ·6H ₂ O, EtOH, NH ₃ solution, Autoclave	Yes (NH ₃)	24 h	180	200-400 nm	Nanoflowers	No
20	<i>J. Mater. Chem. A</i> , 2013, 1 , 830	Wet chemical and hydrothermal	FeCl ₃ and MgCl ₂ , NaOH	No	12 h	130	5-24 nm	Elongated rugby ball-like	No
21	<i>J. Mater. Chem. A</i> , 2013, 1 , 12400	Microwave-assisted hydrothermal method	FeCl ₂ ·4H ₂ O sodium acetate distilled water	No	10 min - 2 h	r.t - 500	50 nm	Nanorods	No
22	<i>Phys. Chem. Chem. Phys.</i> , 2013, 15 , 11717	Electrodeposition and thermally annealed	FeSO ₄ ·7H ₂ O, 98.0% ascorbic acid (C ₆ H ₈ O ₆ , amidosulfonic acid boric acid	No	6 h	500	250-900 nm	Nanosheet	No
23	<i>Cryst. Eng. Comm.</i> , 2013, 15 , 8166	Hydrothermal method followed by annealing	(Fe(ClO ₄) ₃ ·xH ₂ O, NaH ₂ PO ₄ , (NH ₂) ₂ CO, Water	Yes (NaH ₂ PO ₄)	12 h	120	3-5 nm	Spindles	No
24	<i>ACS Appl. Mater. Interfaces</i> , 2013, 5 , 10246	Chemical vapor deposition	Ferrocene and sulphur, Argon, H ₂	Yes (H ₂)	10-30 minutes	1100-1150	<20 nm	Rhombohedral	No
25	<i>Cryst. Eng. Comm.</i> , 2012, 14 , 7701	Biphasic interfacial reaction	Fe(acac) ₃ , urea, PVP, K30, Benzene, Water	No	24 h	130	160–210 nm microstructure	Nanobundle based flower like	No

Table S2: Comparison of present probe **3** for Fe³⁺ ions detection over other reported chemosensors of Fe³⁺ ions reported in the literature:

S. No	System	Utilization of fluorescent nanoaggregates for Fe ³⁺ ions detection	Ratiometric fluorescence response for Fe ³⁺ ions detection	Test strip for detection of trace amount of Fe ³⁺ ions	Detection Limit
1	Present manuscript	Yes	Yes	Yes	64 nM
2	<i>Chem. Commun.</i> , 2014, 50 , 8032	No	Yes	Yes	-
3	<i>J. Mater. Chem. C</i> , 2014, 2 , 5576	No	No (Turn-On Fluorescence response)	No	126 nM
4	<i>Chem. Commun.</i> , 2014, 50 , 4631	No	No (Turn-On Fluorescence response)	No	0.58 μ M
5	<i>Inorg. Chem.</i> , 2014, 53 , 2144	No	No (Turn-On Fluorescence response)	No	4.8 μ M
6	<i>Chem. Commun.</i> , 2013, 49 , 7797	No	Yes	No	1.2 μ M
7	<i>Chem. Commun.</i> , 2013, 49 , 10739	No	No (Turn-On Fluorescence response)	No	10 ⁻⁸ M
8	<i>Chem. Commun.</i> , 2013, 49 , 11557	No	No	No	0.001 M
9	<i>Anal. Chem.</i> 2013, 85 , 7441	No	No. only quenching is observed	No	0.9 μ M
10	<i>ACS Appl. Mater. Interfaces</i> 2013, 5 , 1078	No	No. only quenching is observed	Yes	500 μ M

Table S3: Comparison of catalytic activity α -Fe₂O₃/other iron oxide nanoparticles for the C-C Sonogashira coupling over other reported procedure in literature prepared by derivative **3**.

S. No	Publication	Catalyst used (Nanoparticles)	Use of Pd	Use of CuI	Use of Amine	Reaction time required	Temp. required (in °C)	Isolated Yield (Product, %)
1	Present manuscript	α -Fe ₂ O ₃	No	No	No	24 h	80	84
2	<i>Green Chem.</i> , 2013, 15 , 2132	Fe ₃ O ₄ @Si O ₂ @PPh ₂ @Pd(0)	Yes	No	No	3 h	80	90
3	<i>Adv. Synth. Catal.</i> , 2011, 353 , 125	Fe ₃ O ₄	No	No	No	35 h	125	92
4	<i>Angew. Chem. Int. Ed.</i> 2010, 49 , 1119	Fe ₃ O ₄ @Si O ₂ @PPh ₂ @Pd(0)	Yes	No	No	5 h	60	94
5	<i>Journal of Colloid and Interface Science</i> , 2010, 349 , 613	Pd-Fe	Yes	Yes	No	9 h	80	97
6	<i>ACS Nano</i> , 2009, 3 728	α -Fe ₂ O ₃ Nanopine-Pd	Yes	No	No	45 min	110	85
7	<i>Org. Lett.</i> , 2008, 10 , 3933	Pd/Fe ₃ O ₄	Yes	No	Yes	4 h	130	98
8	<i>Chem. Commun.</i> , 2005, 4435	γ -Fe ₂ O ₃ /NH C-Pd	Yes	Yes	No	12 h	50	90

Table S4: Comparison of present method over other reported procedure in literature for photocatalytic degradation Rhodamine B (RhB) dye by α -Fe₂O₃ nanoparticles prepared by derivative **3**.

S. No	Publication	Degradation time required
1	Present manuscript	26 min
2	<i>Nanoscale</i> , 2014, 6 , 6603	80 min
3	<i>J. Mater. Chem. A</i> , 2013, 1 , 9837	720 min
4	<i>RSC Adv.</i> , 2013, 3 , 7912	4 h
5	<i>Scientific Reports</i> , 2013, DOI: 10.1038/srep02204	100 min
6	<i>Angew. Chem. Int. Ed.</i> , 2012, 51 , 178	80-180 min
7	<i>J. Mater. Chem.</i> , 2012, 22 , 9704	60 min

Table S5: Comparison of catalytic activity α -Fe₂O₃ nanoparticles for the Sonogashira coupling reactions over other noble metal catalysts like Pd, Au, Ag, Ru etc. reported in the literature.

Serial No.	Publication	Catalyst used	Use of Noble metal	Use of CuI	Use of Amine	Solvent	Nano catalysis	Recycling	Reaction time	Temp. required (in °C)	Isolated Yield (Product, %)
1	Present manuscript	α -Fe ₂ O ₃ , K ₂ CO ₃	No	No	No	Ethylene glycol (green solvent)	Yes	Yes	24 h	80	84
2	<i>Angew. Chem. Int. Ed.</i> 2013, 52 , 11554	Pd(0) nanoparticle, KOAc	Yes (Pd)	No	Yes	NMP (toxic)	Yes	No	24 h	160	83
3	<i>Green Chem.</i> , 2013, 15 , 2349	Pd catalyst, K ₂ CO ₃	Yes (Pd)	No	No	EtOH/Chlorobenzene (flammable)	No	Yes	18 h	60	88
4	<i>Green Chem.</i> , 2013, 15 , 2132	Fe ₃ O ₄ @-SiO ₂ @PPh ₂ @Pd(0), NaOH (Very complicated)	Yes (Pd)	No	No	Water	No	Yes	15 min-4 h	80	91
5	<i>J. Mater. Chem. A</i> , 2014, 2 , 484	Pd-PPh ₂ -MCM-41@SiO ₂ @Fe ₃ O ₄ (Very complicated)	Yes (Pd)	No	No	Water	No	Yes	4 h	70	95
6	<i>Chem. Eur. J.</i> 2013, 19 , 14024	5% Pd-Au/C, K ₃ PO ₄	Yes (Pd, Au)	No	No	<i>i</i> PrOH/H ₂ O	No	No	20 h	80	73
7	<i>Chem. Commun.</i> , 2010, 46 , 6524	Pd@meso-SiO ₂ (Very complicated)	Yes (Pd)	No	No	EtOH	No	Yes	30 h	80	55
8	<i>Angew. Chem. Int. Ed.</i> 2007, 46 , 1536	Au(I), K ₃ PO ₄	Yes (Au)	No	No	<i>O</i> -Xylene	No	No	24 h	130	54
9	<i>Langmuir</i> , 2010, 14 , 12225	Au-Ag-Pd trimetallic nanoparticles	Yes (Pd, Au, Ag)	No	No	DMF-H ₂ O	No	No	2 h	120	94
10	<i>Org. Lett.</i> , 2 , 2000, 2935	Pd(PPh ₃) ₂ , Ag ₂ O	Yes (Pd, Ag)	No	No	THF	No	No	8 h	60	60
11	<i>J. Comb. Chem.</i> 2004, 6 , 297	RuCl ₂ (1-Me,4- <i>i</i> PrC ₆ H ₄)(PPh ₃)	Yes (Ru)	Yes	Yes	THF	No	No	20 h	50	10-100 (GC-Mass)

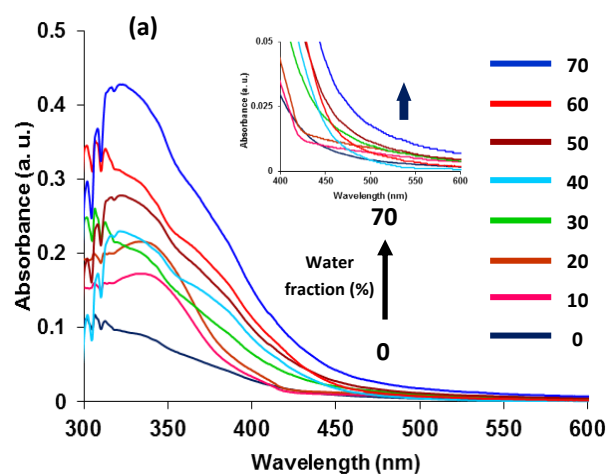


Fig. S1A: UV-vis spectrum showing the change in absorbance of compound **3** (5 μM) in Water/Ethanol mixture (0 to 70% volume fraction of water in Ethanol).

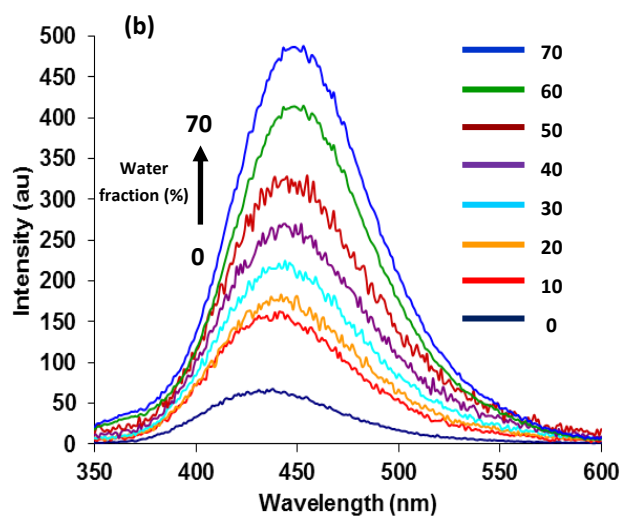


Fig. S1B: Fluorescence spectra of compound **3** (5 μM) showing the variation of fluorescence intensity in Water/Ethanol mixture (0 to 70% volume fraction of water in Ethanol); λ_{ex} = 320 nm.

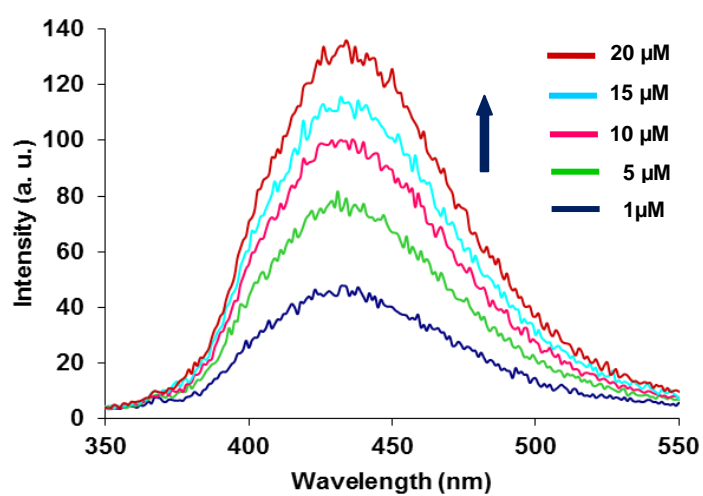


Fig. S2: Fluorescence spectra of compound **3** showing the variation of fluorescence intensity with different concentration of **3** (1 μM - 20 μM) in ethanol; λ_{ex} = 320 nm

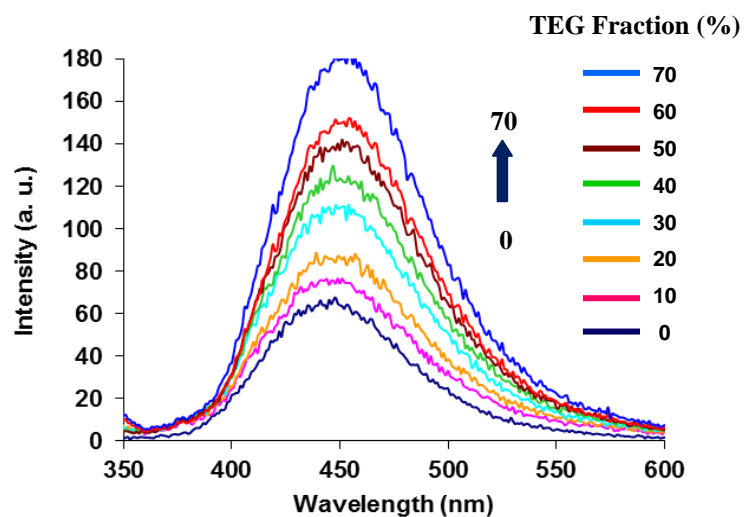


Fig. S3A: Fluorescence spectra of compound **3** (5 μ M) showing the variation of fluorescence intensity in TEG/EtOH mixture (0 to 70% volume fraction of TEG in Ethanol); λ_{ex} = 320 nm.

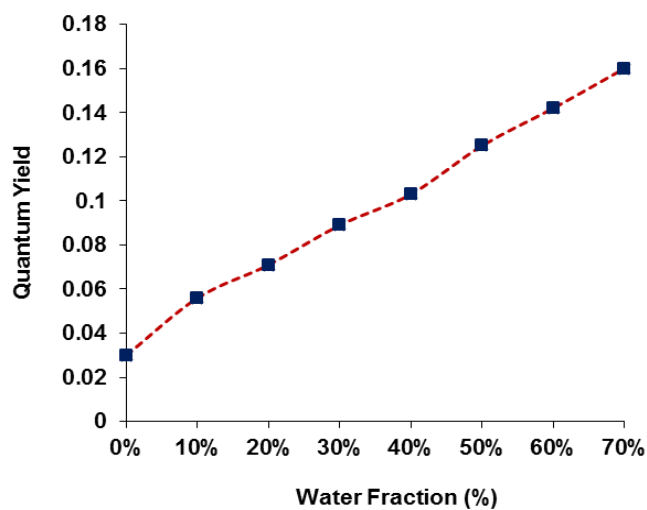


Fig. S3B: Variation in quantum yield value with the variation of water fractions (0 to 70% volume fraction of water in Ethanol); λ_{ex} = 320 nm.

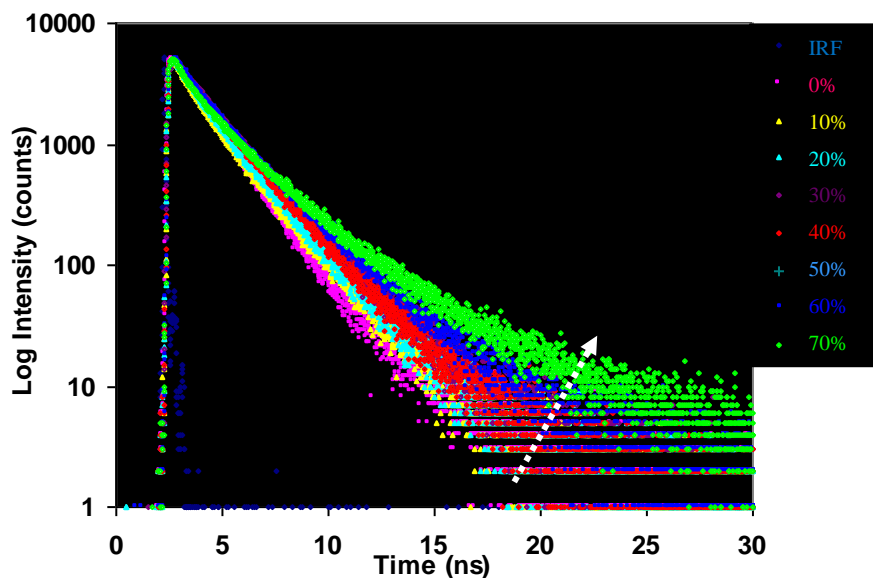


Fig. S4: Exponential fluorescence decays of **3** on addition of water fraction measured at 455 nm. Spectra were acquired in Water/Ethanol mixture (0 to 70% volume fraction of water in Ethanol), $\lambda_{\text{ex}} = 377$ nm.

Water fraction %	Quantum Yield (Φ_f)	A_1/A_2	τ_1 (ns)	τ_2 (ns)	τ_{avg} (Average lifetime, ns)	K_f (10^9 s^{-1})	K_{nr} (10^9 s^{-1})
0	0.03	65/35	0.08	1.33	0.2	0.15	4.85
70	0.16	10/90	0.57	1.67	1.41	0.113	0.59

Table S6: Fluorescence lifetime of derivative **3** in absence and presence of water (70%) in EtOH at 455 nm. A_1 , A_2 : fractional amount of molecules in each environment. τ_1 , τ_2 and τ_{avg} : bi-exponential and average life time of aggregates in 70 vol% of water in EtOH; K_f : radiative rate constant ($K_f = \Phi_f/\tau_{\text{avg}}$); K_{nr} : non-radiative rate constant ($K_{\text{nr}} = (1 - \Phi_f)/\tau_{\text{avg}}$); $\lambda_{\text{ex}} = 377$ nm.

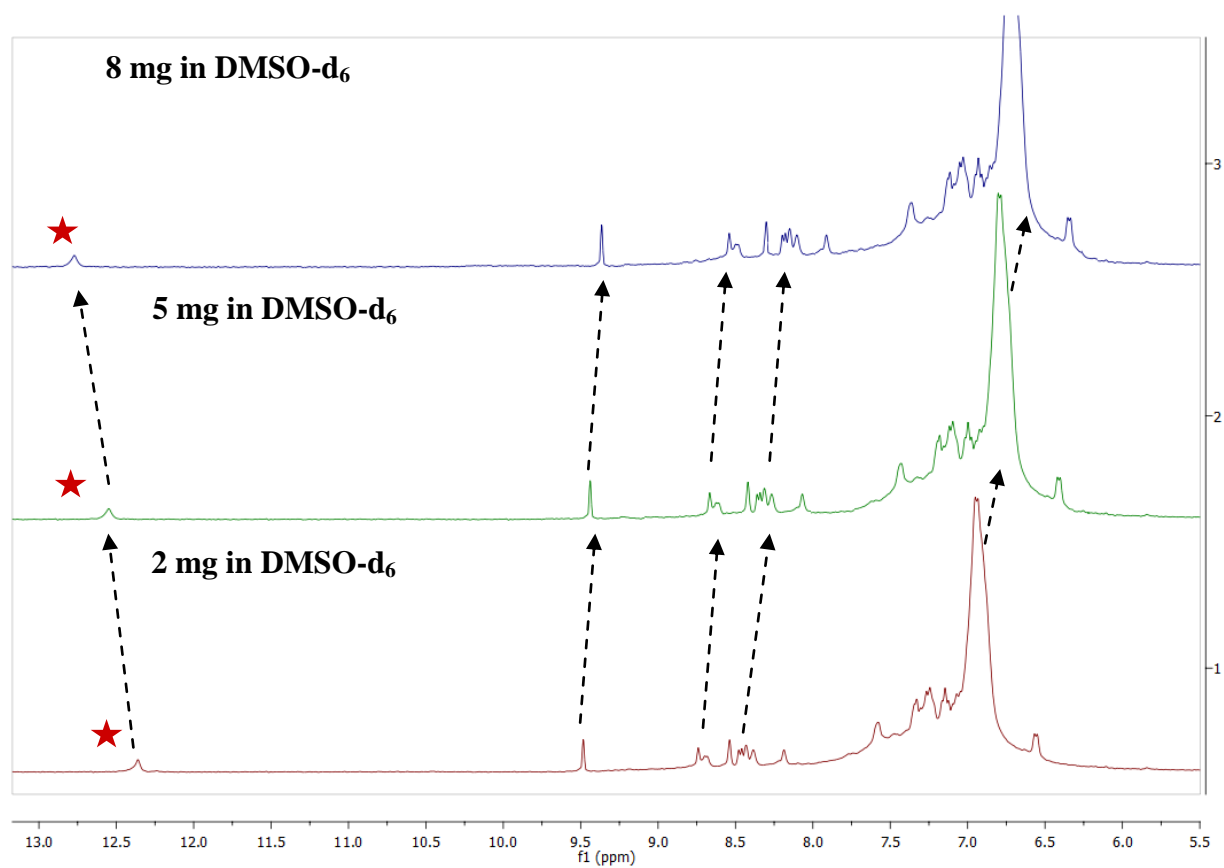


Fig. S6: Concentration dependent ^1H NMR spectra of compound **3** in 500 μl DMSO-d_6 .

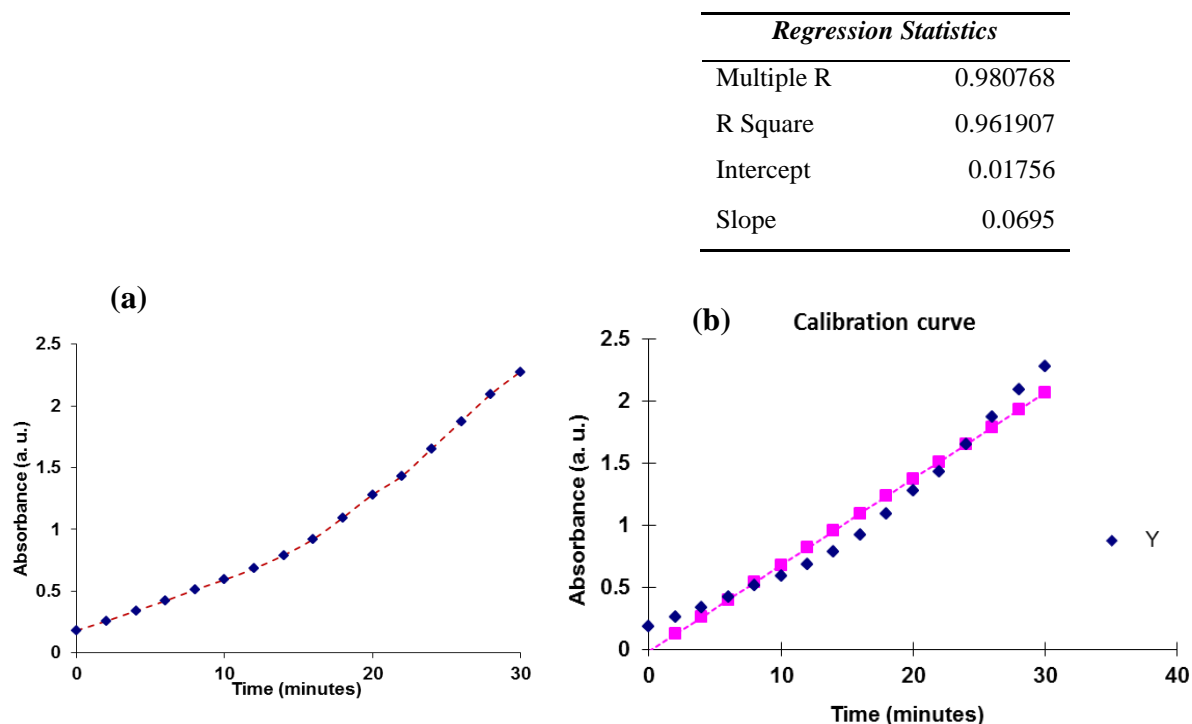


Fig. S7: Graphical representation of the rate of formation of α -Fe₂O₃ nanoparticles of derivative **3**. (a) Time (min.) vs. absorbance plot at 395 nm (b) regression plot of a.

The first order rate constant for the formation of iron oxide nanoparticles was calculated from the changes of intensity of absorbance of aggregates of derivative **3** in the presence of Fe³⁺ ions at different time interval.

From the time vs. absorbance plot at fixed wavelength 395 nm by using first order rate equation we get the rate constant = $k = \text{slope} \times 2.303 = 0.0695 \times 2.303 = 2.66 \times 10^{-3} \text{ Sec}^{-1}$.

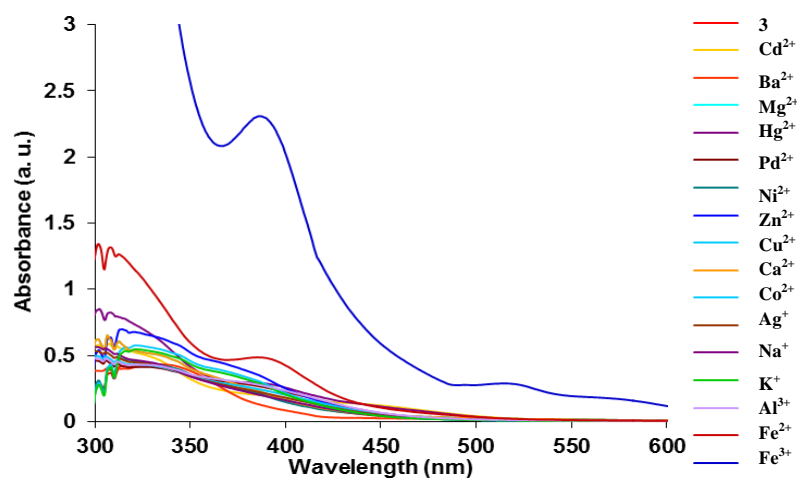


Fig. S8A: UV-vis spectra of derivative **3** (5 μM) upon additions of 50 μM of various metal ions as their chloride salt in in $\text{H}_2\text{O}/\text{EtOH}$ (7:3, v/v) mixture.

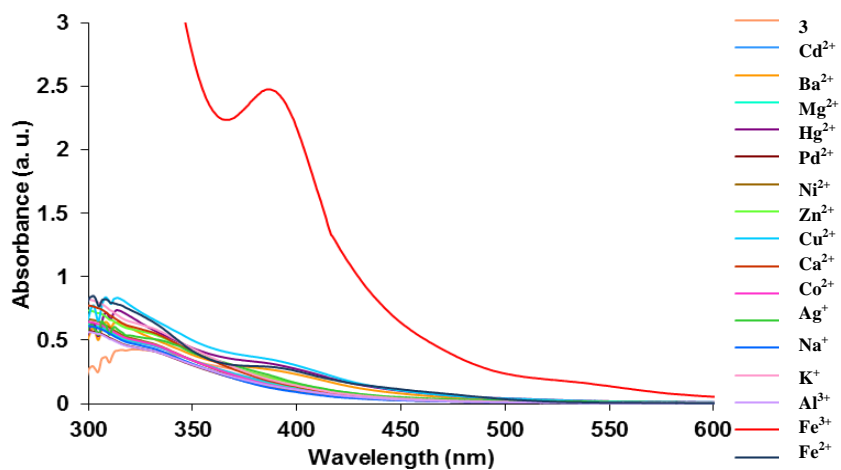


Fig. S8B: UV-vis spectra of derivative **3** (5 μM) upon additions of 50 μM of various metal ions as their perchlorate salt in in $\text{H}_2\text{O}/\text{EtOH}$ (7:3, v/v) mixture.

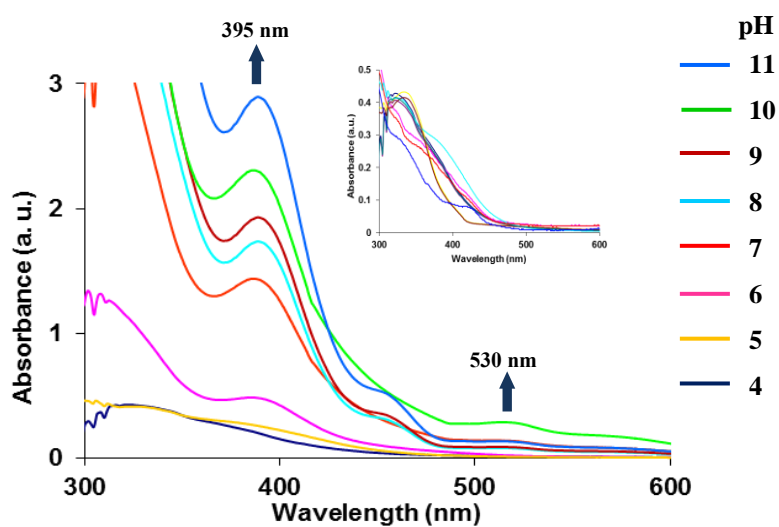


Fig. S9: UV-vis spectra of compound **3** (5 μM) showing the variation after 5 minutes of addition of Fe^{3+} ions (0-25 equiv.) in $\text{H}_2\text{O}/\text{EtOH}$ (7:3, v/v) mixture at different pH solutions; Inset showing there is no variation in the absorbance of compound **3** (5 μM) with the variation of different pH solutions in $\text{H}_2\text{O}/\text{EtOH}$ (7:3, v/v) mixture.

<i>Regression Statistics</i>	
Multiple R	0.980854
R Square	0.962074
Stern-Volmer	
constant =	$6.08 \times 10^4 \text{ M}^{-1}$

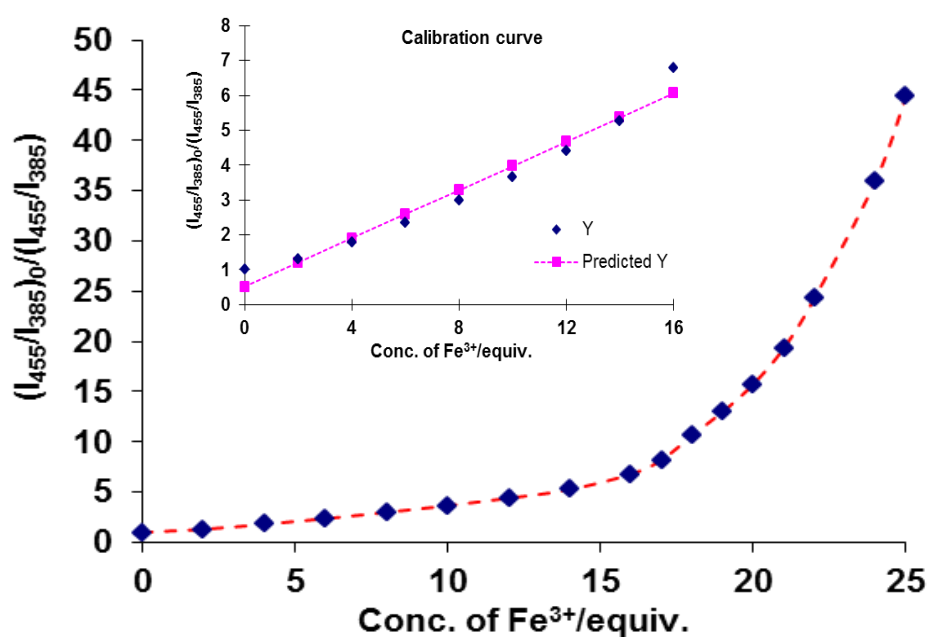


Fig. S10: Plot of fluorescence quenching efficiency of the ratiometric probe **3** (5 μM) as a function of the Fe^{3+} ions concentration. $(I_{455}/I_{385})_0$ and (I_{455}/I_{385}) were the ratio of the fluorescence intensity of the ratiometric probe in the absence and presence of different concentrations of Fe^{3+} ions, respectively; Inset showing the regression curve.

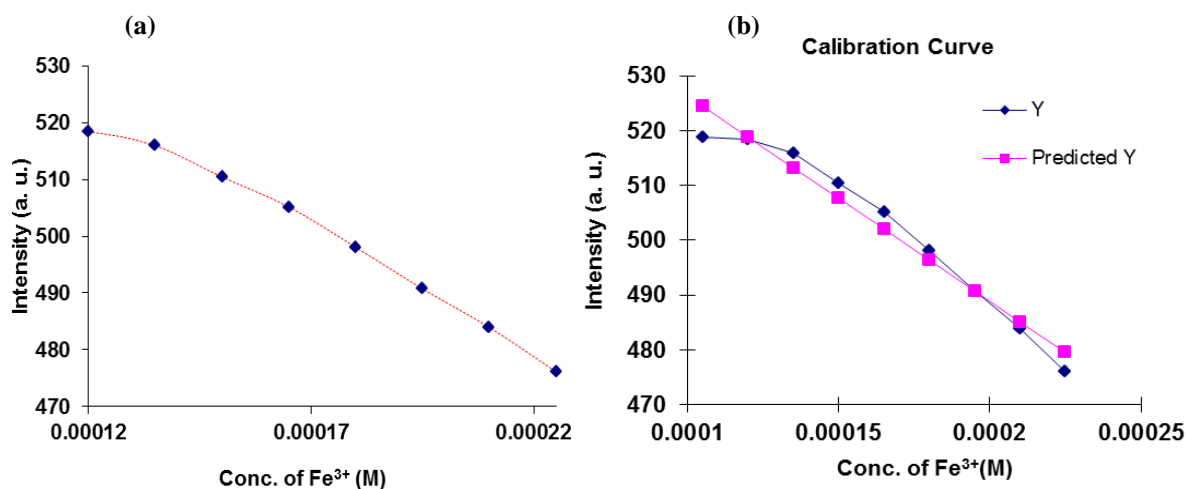


Fig. S11: (a) Showing the fluorescence intensity of compound **3** and (b) Calibrated curve showing the fluorescence intensity of compound **3** at 380 nm as a function of Fe³⁺ ions concentration (equiv.) in H₂O/EtOH (7:3, v/v) buffered with HEPES, pH = 7.05, λ_{ex} = 320 nm.

Multiple R = 0.98135,

R² = 0.96305,

Standard deviation = 0.008,

Observation = 10,

Intercept = 563.80,

Slope = 374700

The detection limit was calculated based on the fluorescence titration. To determine the S/N ratio, the emission intensity of receptor **3** without Fe³⁺ was measured by 10 times and the standard deviation of blank measurements was determined. The detection limit is then calculated with the following equation:

$$DL = 3 \times SD/S$$

Where SD is the standard deviation of the blank solution measured by 10 times; S is the slope of the calibration curve.

From the graph we get slope

S = 374700, and SD value is 0.008

Thus using the formula we get the Detection Limit (DL) = $3 \times 0.008/374700 = 64 \times 10^{-9} \text{ M}$

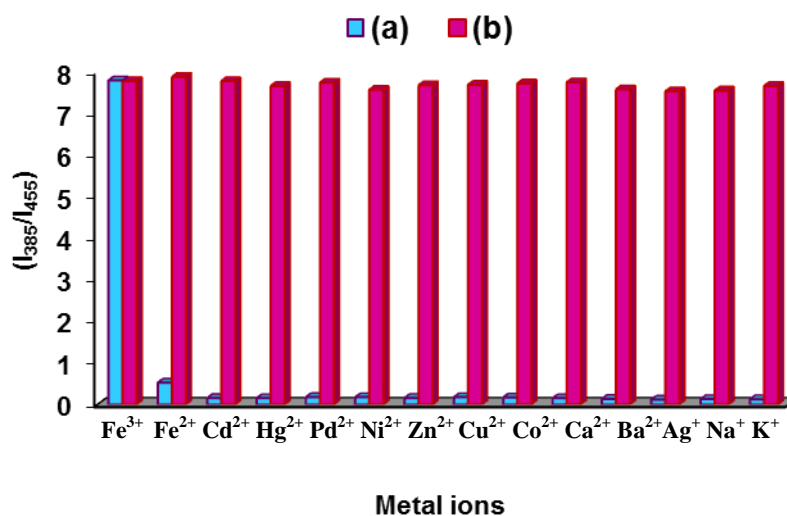


Fig. S12A: Fluorescence response of **3** (5.0 μM) to various metal ions of **chloride salts** (25 equiv) in H₂O/EtOH (7:3, v/v) mixture buffered with HEPES; pH = 7.05; λ_{ex} = 320 nm. Bars represent the emission intensity ratio (I₃₈₅/I₄₅₅) (I₄₅₅ = initial fluorescence intensity at 455 nm; I₃₈₅ = final fluorescence intensity at 385 nm after the addition of metal ions). (a) Blue bars represent selectivity (I₃₈₅/I₄₅₅) of **3** upon addition of different anions. (b) Pink bars represent competitive selectivity of receptor **3** toward Fe³⁺ ions (25 equiv.) in the presence of other metal ions (100 equiv.).

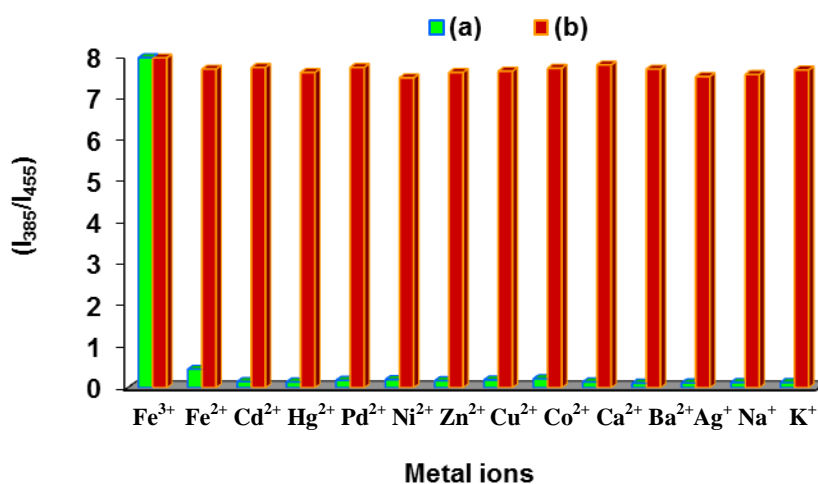


Fig. S12B: Fluorescence response of **3** (5.0 μM) to various metal ions of **perchlorate salts** (25 equiv) in H₂O/EtOH (7:3, v/v) mixture buffered with HEPES; pH = 7.05; λ_{ex} = 320 nm. Bars represent the emission intensity ratio (I₃₈₅/I₄₅₅) (I₄₅₅ = initial fluorescence intensity at 455 nm; I₃₈₅ = final fluorescence intensity at 385 nm after the addition of metal ions). (a) Green bars represent selectivity (I₃₈₅/I₄₅₅) of **3** upon addition of different anions. (b) Red bars represent competitive selectivity of receptor **3** toward Fe³⁺ ions (25 equiv.) in the presence of other metal ions (100 equiv.).

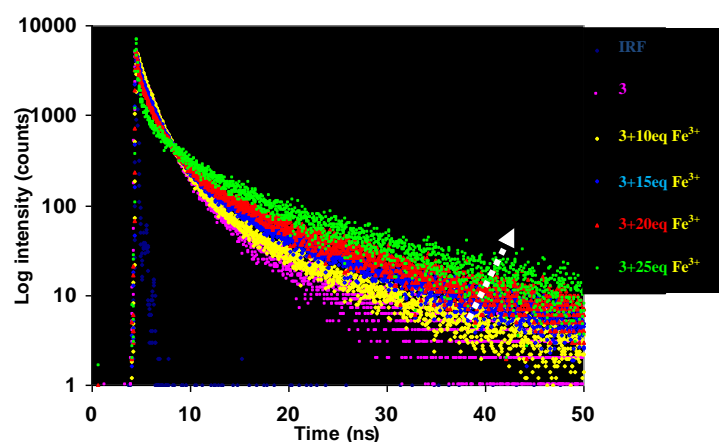


Fig. S13: Exponential fluorescence decays of **3** on addition of different amount of Fe^{3+} ions within 30 minutes measured at 385 nm. Spectra were acquired in $\text{H}_2\text{O}/\text{EtOH}$ (7:3, v/v) mixture, $\lambda_{\text{ex}} = 377$ nm.

Fe^{3+} (equiv.)	Quantum Yield	A_1/A_2	τ_1 (ns)	τ_2 (ns)	τ_{avg} (Average lifetime, ns)	K_f (10^9 s^{-1})	K_{nr} (10^9 s^{-1})
0	0.16	95/5	0.27	1.55	0.55	0.29	1.52
25	0.14	45/55	0.57	1.78	1.35	0.104	0.63

Table S7: Fluorescence lifetime of derivative **3** in absence and presence of Fe^{3+} ions (25 equiv.; 30 minutes) in $\text{H}_2\text{O}/\text{EtOH}$ (7:3, v/v) mixture buffered with HEPES; pH = 7.05; at 385 nm. A_1 , A_2 : fractional amount of molecules in each environment. τ_1 and τ_2 : biexponential life time of aggregates in 70 vol% of water in EtOH; K_f : radiative rate constant ($K_f = \Phi_f/\tau_{\text{avg}}$); K_{nr} : non-radiative rate constant ($K_{\text{nr}} = (1 - \Phi_f)/\tau_{\text{avg}}$); $\lambda_{\text{ex}} = 377$ nm.

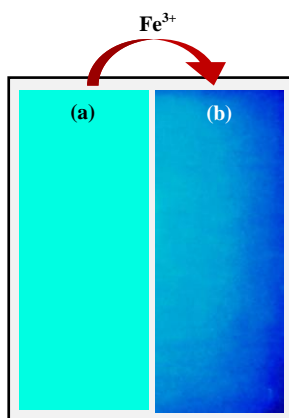


Fig. S14A: Photographs (under 365 nm UV light with naked eye) of compound **3** on test strips (a) before and (b) after dipping into aqueous solution of Fe^{3+} ions (10^{-3} M).

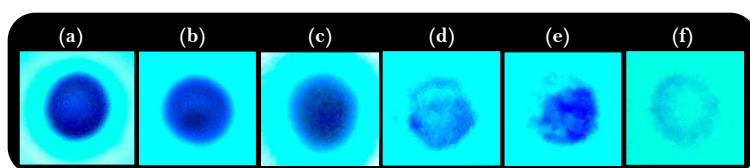


Fig. S14B: Paper strips of **3** showing the change in the fluorescence on addition of Fe^{3+} ions in aqueous medium at different concentrations of Fe^{3+} ions (a) 10^{-1} M, (b) 10^{-2} M, (c) 10^{-3} M, (d) 10^{-4} M, (e) 10^{-5} M, (f) 10^{-6} M (under 365 nm UV light).

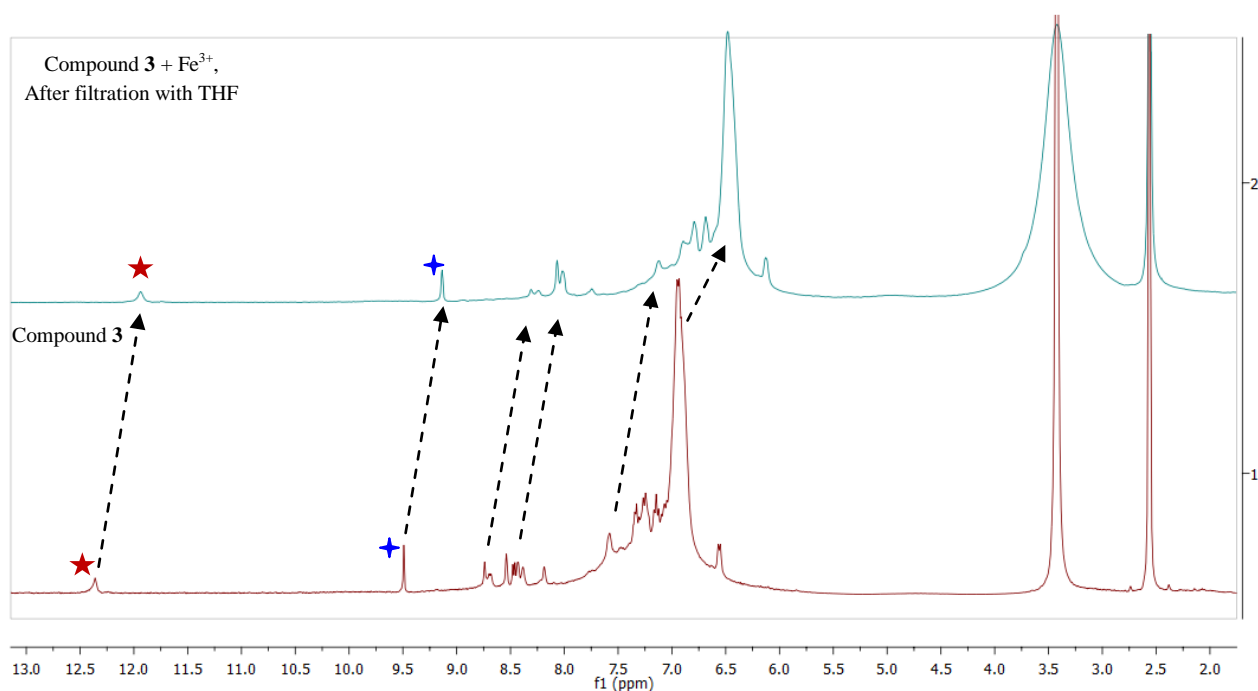


Fig. S15: Overlay ^1H NMR spectra of derivative **3** in DMSO-d_6 and $\alpha\text{-Fe}_2\text{O}_3$ nanoparticles of derivative **3** after filtration with THF.

Compound 3 (δ_3 , ppm)	Compound 3 + Fe^{3+} , After filtration by THF (δ_F , ppm)	$\Delta\delta_1 = \delta_3 - \delta_F$
★ 12.36 (-NH)	11.92	0.44
★ 9.46 (-N=CH)	9.15	0.31
8.69 (d, aromatic)	8.28	0.41
8.48-8.38 (m, aromatic)	8.10-8.06	0.38
8.19 (s, aromatic)	7.72	0.47
7.34 (d, aromatic)	7.15	0.19
7.26 (d, aromatic)	6.82	0.44
7.15 (t, aromatic)	6.78	0.37
7.06 (d, aromatic)	6.65	0.41
6.95-6.91 (m, aromatic)	6.52-6.48	0.43
6.56 (d, aromatic)	6.18	0.38

Table S8: Change in chemical shift (δ) value of ^1H NMR spectra of derivative **3** in DMSO-d_6 and $\alpha\text{-Fe}_2\text{O}_3$ nanoparticles of derivative **3** after filtration with THF.

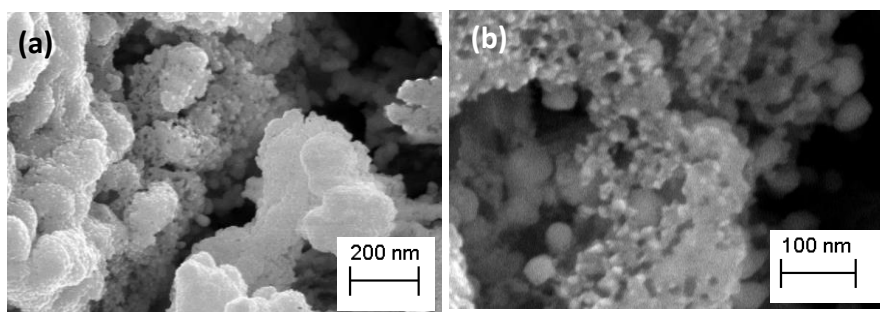


Fig. S16A: Photographs of SEM images (a-b) showing aggregates of **3** in H₂O/EtOH (7:3, v/v) after treatment of FeCl₃ with compound **3**.

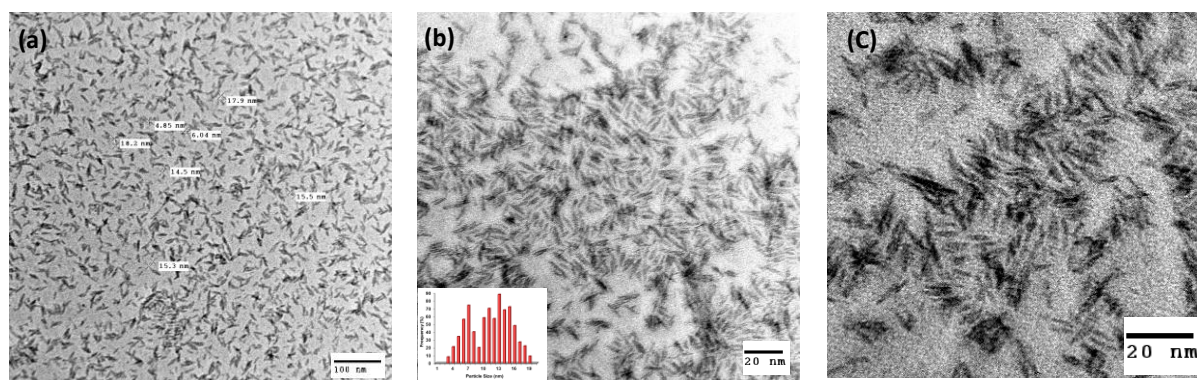


Fig. S16B: (a-c) The TEM images of α -Fe₂O₃ Nanorods and inset of b showing size distribution of these nanoparticles.

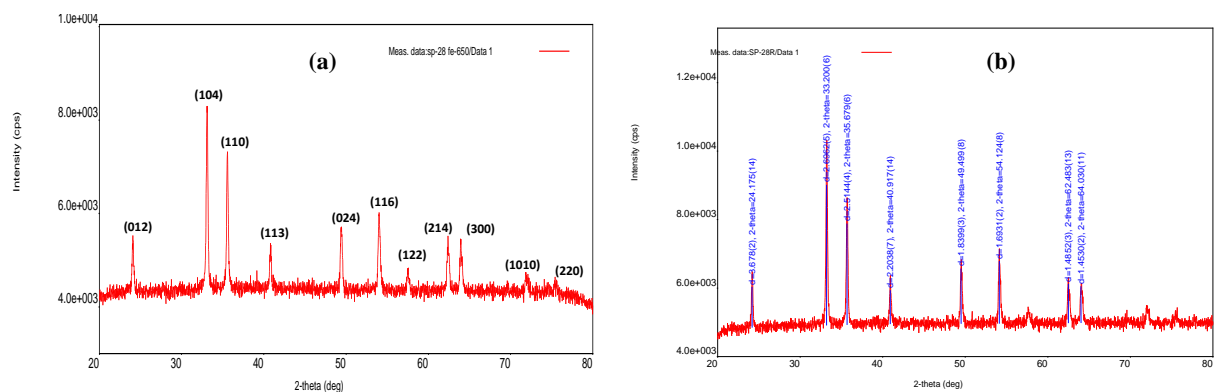


Fig. S17A: (a-b) Representative XRD diffraction patterns of α -Fe₂O₃ nanoparticles prepared by derivative 3.

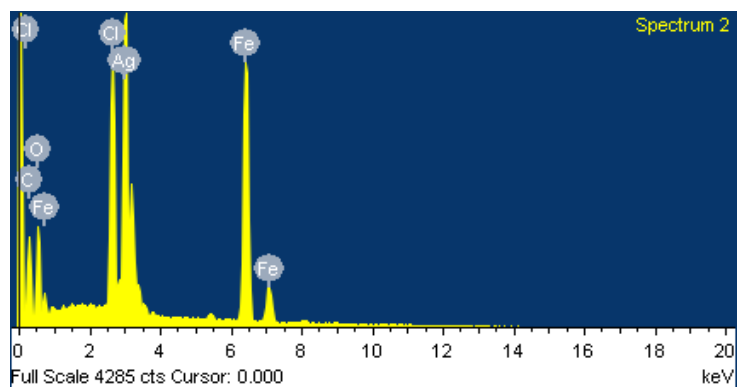


Fig. S17B: EDX spectra of α -Fe₂O₃-nanoparticles of derivative 3

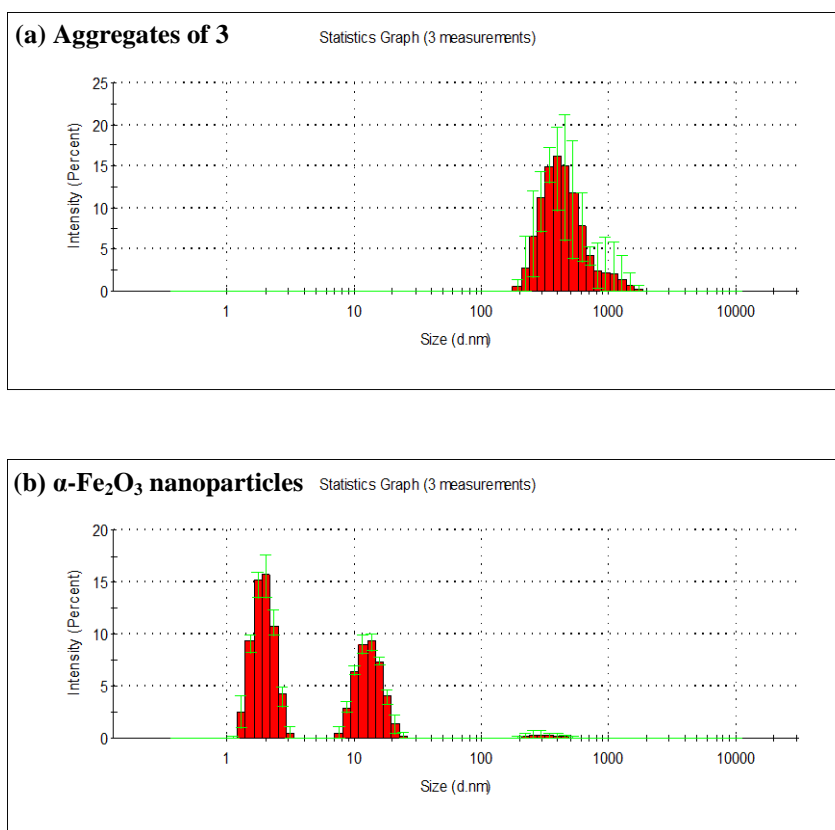
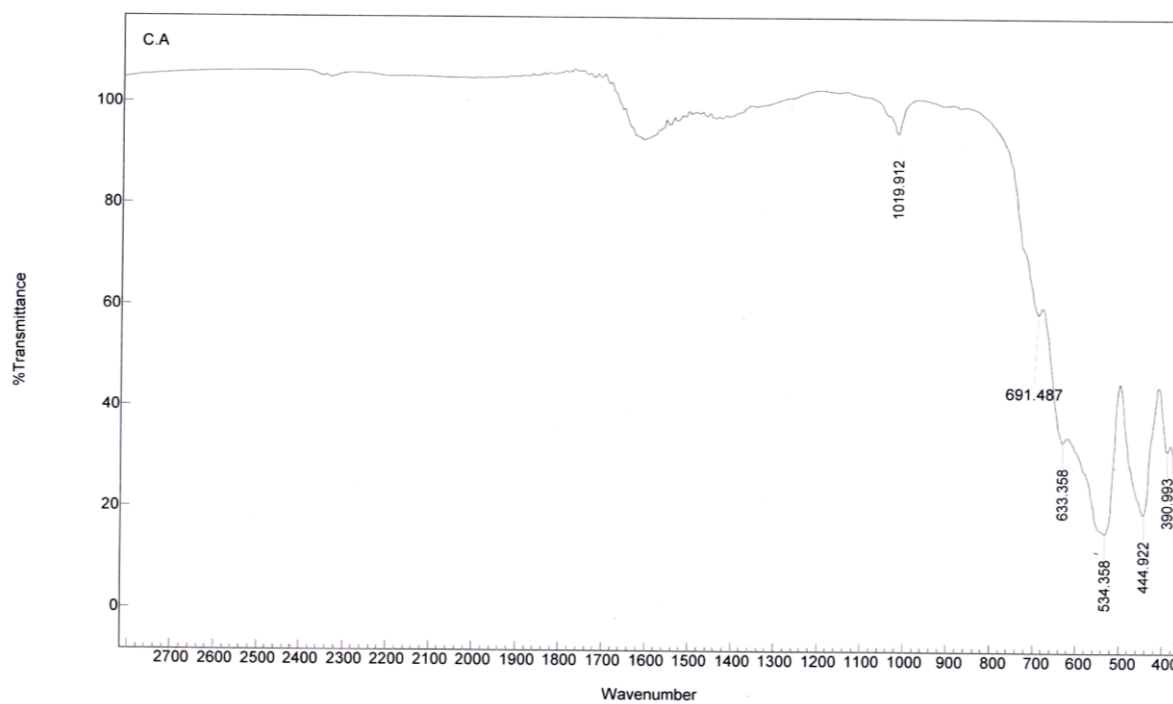
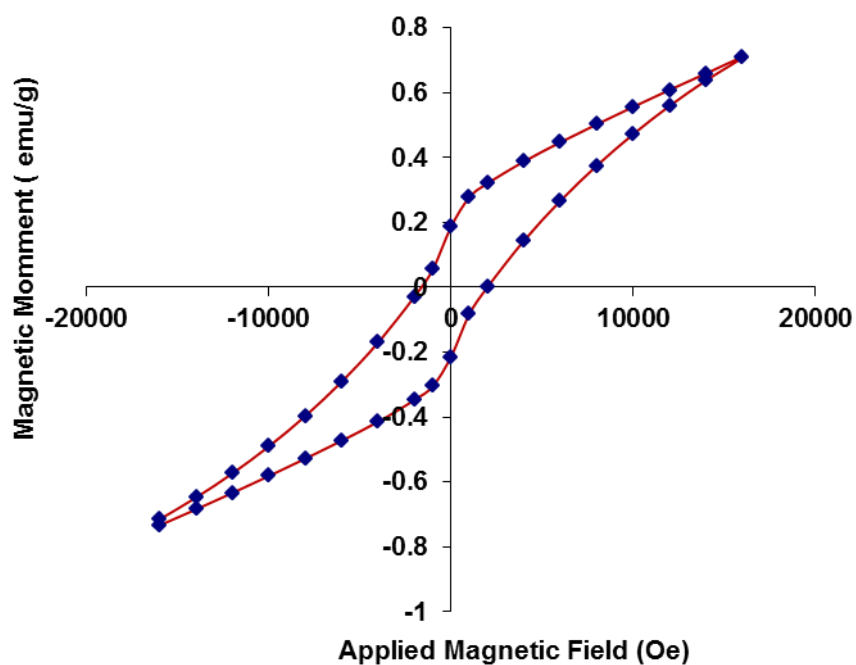


Fig. S18: Dynamic light scattering (DLS) results showing the particle size diameter (a) aggregates of **3** in H₂O/EtOH (7:3, v/v) mixture and (b) α -Fe₂O₃ nanoparticles prepared by aggregates of **3**.

Fig. S19: FT-IR Spectrum of α -Fe₂O₃ nanoparticles:

Agilent Resolutions Pro





Parameters

	Upward Part	Downward part	Average	Parameter 'definition'
Hysteresis Loop				Hysteresis Parameters
Hc Oe	1996.067	-1661.297	1828.682	Coercive Field: Field at which M/H changes sign
Mr emu	-25.694E-3	22.339E-3	24.016E-3	Remanent Magnetization: M at H=0
S	0.302	0.254	0.278	Squareness: Mr/Ms
S*	0.172	0.568	0.370	1-(Mr/Hc)/(1/slope at Hc)
Ms emu	84.990E-3	-88.035E-3	86.513E-3	Saturation Magnetization: maximum M measured
M at H max emu	84.990E-3	-85.789E-3	85.390E-3	M at the maximum field

Fig. S20: Hysteresis loops of α -Fe₂O₃ nanoparticles at room temperature, 25°C.

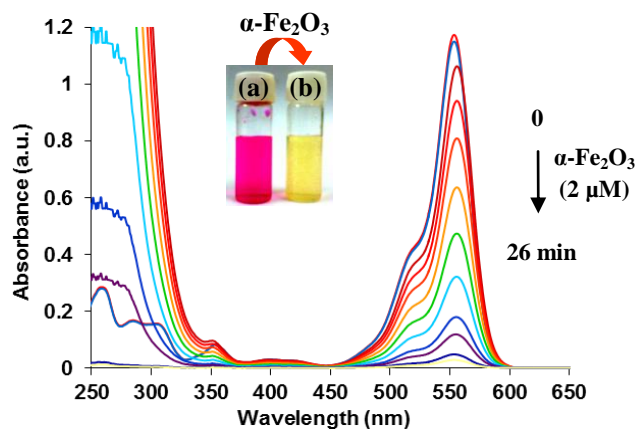


Fig. S21A Changes of time-dependent UV-Vis absorbance spectra of RhB solutions (0.1 mM) in the presence of $\alpha\text{-Fe}_2\text{O}_3$ nanoparticle (2 μM) with 2 mM H_2O_2 under visible-light irradiation for different time interval and (inset) photographs of the corresponding color change of RhB solutions from red to colourless (a) before and (b) after 26 minutes of $\alpha\text{-Fe}_2\text{O}_3$ addition.

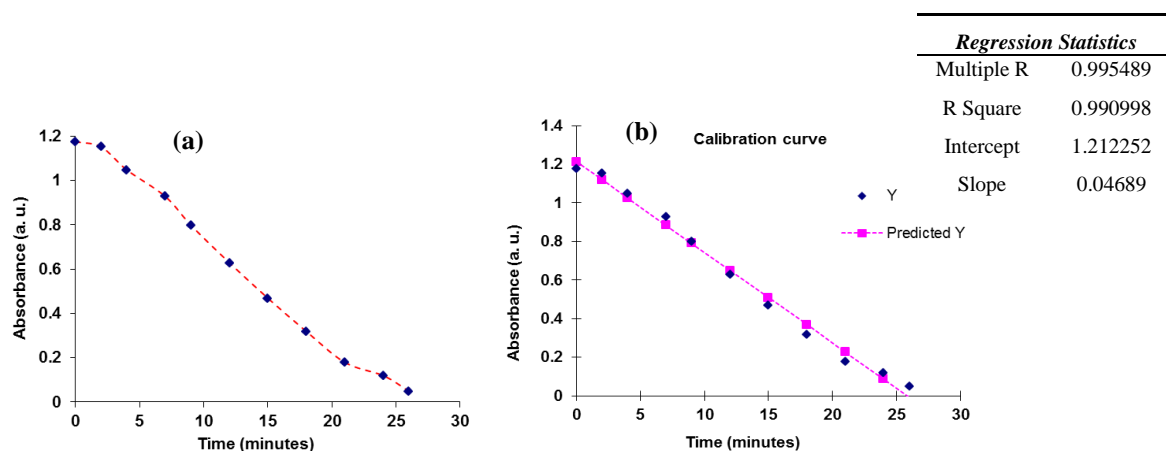
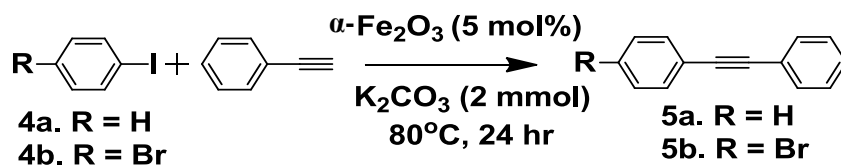


Fig. S21B. The rate of photo catalytic degradation of the aqueous solution RhB dye by $\alpha\text{-Fe}_2\text{O}_3$ nanoparticles in presence of 2 mM H_2O_2 (a) Time (min.) vs. absorbance plot at 555 nm (b) Calibration curve regression plot of A.

The first order rate constant of photo catalytic degradation of the aqueous solution RhB dye by iron oxide nanoparticles was calculated from the changes of intensity of absorbance of RhB dye by $\alpha\text{-Fe}_2\text{O}_3$ nanoparticles at different time interval.

From the time vs. absorbance plot at fixed wavelength 555 nm by using first order rate equation we get the rate constant = $k = \text{slope} \times 2.303 = 0.04689 \times 2.303 = 1.79 \times 10^{-3} \text{ Sec}^{-1}$

Catalytic applications: Sonogashira Cross Coupling reactions



Scheme 2. Synthesis of hexaphenylbenzene based derivative **3**.

Table S9: The isolated yield of product formation in various solvent

Entry	Solvent	Isolated yield [%]
5a	EG	84
	DMF	63
5b	EG	78
	DMF	56

Synthesis of Compound **5a**:

The reaction of iodobenzene (204 mg, 1 mmol) with phenylacetylene (100 mg, 1 mmol) as a model reaction in the presence of K_2CO_3 (276 mg, 2 mmol) and 5 mol% of the Nano catalyst ($\alpha\text{-Fe}_2\text{O}_3$) at 80°C was studied to furnished white crystalline **5a** in 84% (150 mg) yield (Scheme 2). The structure of compound **5a** was confirmed from its spectroscopic and analytical data (Fig. S22-S23, ESI[†]). ^1H NMR (500 MHz, CDCl_3 , ppm) δ = 7.60-7.58 (m, 4H, ArH), 7.41-7.36 (m, 6H, ArH). ^{13}C NMR (125 MHz, CDCl_3 , ppm) δ = 131.64, 128.38, 128.28, 123.31, 89.41. ESI-MS mass spectrum of compound **5a** showed a parent ion peak, m/z = 179.0805 $[\text{M}+\text{H}]^+$.

Synthesis of Compound **5b**:

The reaction of 1-bromo-4-iodobenzene (282 mg, 1 mmol) with phenylacetylene (100 mg, 1 mmol) as a model reaction in the presence of K_2CO_3 (276 mg, 2 mmol) and 5 mol% of the Nano catalyst ($\alpha\text{-Fe}_2\text{O}_3$) at 80°C was studied to furnished white crystalline **5b** in 78% (200 mg) yield (Scheme 2). The structure of compound **5b** was confirmed from its spectroscopic and analytical data (Fig. S24-S25, ESI[†]). ^1H NMR (500 MHz, CDCl_3 , ppm) δ = 7.57-7.55 (m, 2H, ArH), 7.51 (d, J = 10 Hz, 2H, ArH), 7.42 (d, J = 10 Hz, 2H, ArH), 7.39-7.38 (m, 3H, ArH). ^{13}C NMR (125 MHz, CDCl_3 , ppm) δ = 133.04, 132.52, 131.63, 129.22, 128.42, 122.93, 122.27, 90.53, 88.32. ESI-MS mass spectrum of compound **5b** showed a parent ion peak, m/z = 257.0334 $[\text{M}+\text{H}]^+$.

Table S10a: Comparison of catalytic activity α -Fe₂O₃ nanoparticles for the mentioned Sonogashira coupling (**5a**) over other reported procedure in literature.


Compound	Serial No.	Publication	Catalyst used	Use of Noble metal	Use of CuI	Use of Amine	Solvent	Nano catalysis	Recycling	Reaction time required	Temp. required (in °C)	Isolated Yield (Product, %)
 5a	1	Present manuscript	α -Fe ₂ O ₃ , K ₂ CO ₃	No	No	No	Ethylene glycol (Green Solvent)	Yes	Yes	24 h	80	84
	2	<i>Angew. Chem. Int. Ed.</i> 2013, 52 , 11554	Pd(0) nanoparticle, KOAc	Yes (Pd)	No	Yes	NMP (Toxic)	Yes	No	24 h	160	83
	3	<i>Green Chem.</i> , 2013, 15 , 2349	Pd catalyst, K ₂ CO ₃	Yes (Pd)	No	No	EtOH/Chlorobenzene (flammable)	No	Yes	18 h	60	88
	4	<i>Green Chem.</i> , 2013, 15 , 2132	Fe ₃ O ₄ @-SiO ₂ @PPh ₂ @Pd(0), NaOH (Very complicated)	Yes (Pd)	No	No	Water	No	Yes	15 min-4 h	80	91
	5	<i>J. Mater. Chem. A</i> , 2014, 2 , 484	Pd-PPh ₂ -MCM-41@SiO ₂ @Fe ₃ O ₄ (Very complicated)	Yes (Pd)	No	No	Water	No	Yes	4 h	70	95
	6	<i>Chem. Eur. J.</i> 2013, 19 , 14024	5% Pd-Au/C, K ₃ PO ₄	Yes (Pd, Au)	No	No	<i>i</i> PrOH/H ₂ O	No	No	20 h	80	73
	7	<i>Tetrahedron Lett.</i> , 2014, 55 , 2256	PVC-Pd(0), NMP	Yes (Pd)	No	Yes	NMP	No	Yes	3-4 h	r. t.	93
	8	<i>Chem. Commun.</i> , 2010, 46 , 6524	Pd@meso-SiO ₂ (Very complicated)	Yes (Pd)	No	No	EtOH	No	Yes	30 h	80	55
	9	<i>Langmuir</i> , 2010, 14 , 12225	Au-Ag-Pd trimetallic nanoparticles	Yes (Pd, Au, Ag)	No	No	DMF-H ₂ O	No	No	2 h	120	94

Table S10b: Comparison of catalytic activity α -Fe₂O₃ nanoparticles for the mentioned Sonogashira coupling (**5b**) over other reported procedure in literature.

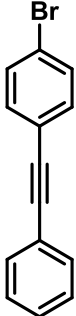
Compound	Serial No.	Publication	Catalyst used	Use of Noble metal	Use of CuI	Use of Amine	Solvent	Nano catalysis	Recycling	Reaction time required	Temp. required (in °C)	Isolated Yield (Product, %)
 5b	1	Present manuscript	α -Fe ₂ O ₃ , K ₂ CO ₃	No	No	No	Ethylene glycol	Yes	Yes	24 h	80	78
	2	<i>J. Organomet. Chem.</i> , 2014, 749 , 405	PS-triazine-Pd(II), Et ₃ N	Yes	No	Yes	Et ₃ N	No	No	3 h	Room temp.	50
	3	<i>Adv. Synth. Catal.</i> , 2013, 18 , 3648	Pd nanoparticle, <i>t</i> -BuOK	Yes	No	No	Glycerol	No	No	2 h	100	91
	4	<i>J. Org. Chem.</i> , 2013, 78 , 12703	Pd(OAc) ₂ , PPh ₃ , CuI, Et ₃ N	Yes	Yes	Yes	Et ₃ N	No	No	1 h	Room temp.	70
	5	<i>Adv. Synth. Catal.</i> , 2012, 8 , 1542	Pd(PPh ₃) ₂ Cl ₂ , CuI, Et ₃ N, THF	Yes	Yes	Yes	Et ₃ N	No	No	24 h	Room temp.	86
	6	<i>Adv. Funct. Mater.</i> , 2012, 10 , 2015	Pd(PPh ₃) ₂ Cl ₂ , CuI, Et ₃ N	Yes	Yes	Yes	Et ₃ N	No	No	24 h	Room temp.	90
	7	<i>J. Am. Chem. Soc.</i> , 2011, 51 20962	Pd(PPh ₃) ₂ Cl ₂ , CuI, Et ₃ N, THF	Yes	Yes	Yes	THF	No	No	24	Room temp.	28
	8	<i>Macromolecules</i> 1998, 31 , 6014	Pd(PPh ₃) ₄ , CuI, Piperidine	Yes	Yes	Yes	Piperidine	No	No	24 h	Room temp.	82

Fig. S22A: ^1H NMR Spectra (CDCl_3 , 500 MHz, ppm) of compound 5a:

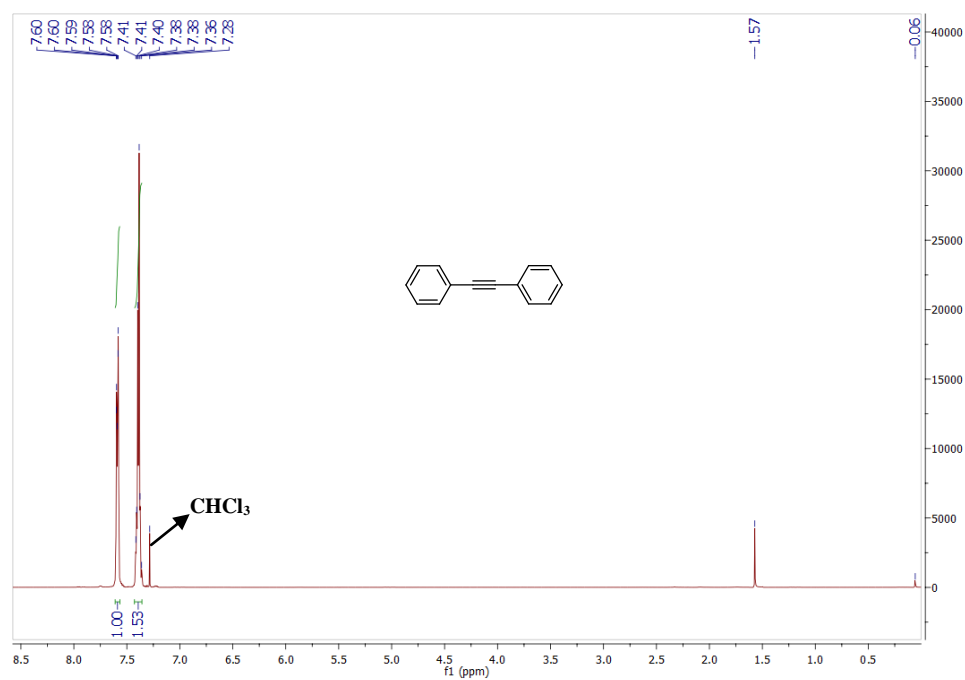


Fig. S22B: ^{13}C NMR Spectra (CDCl_3 , 500 MHz, ppm) of compound 5a:

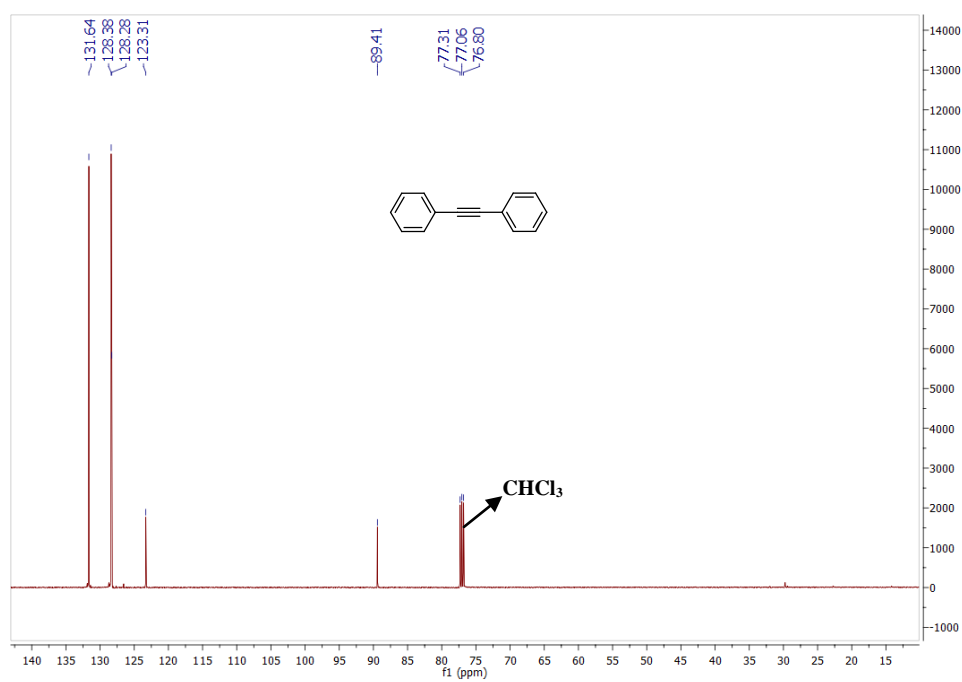


Fig. S23: ESI-MS Spectrum of compound 5a:

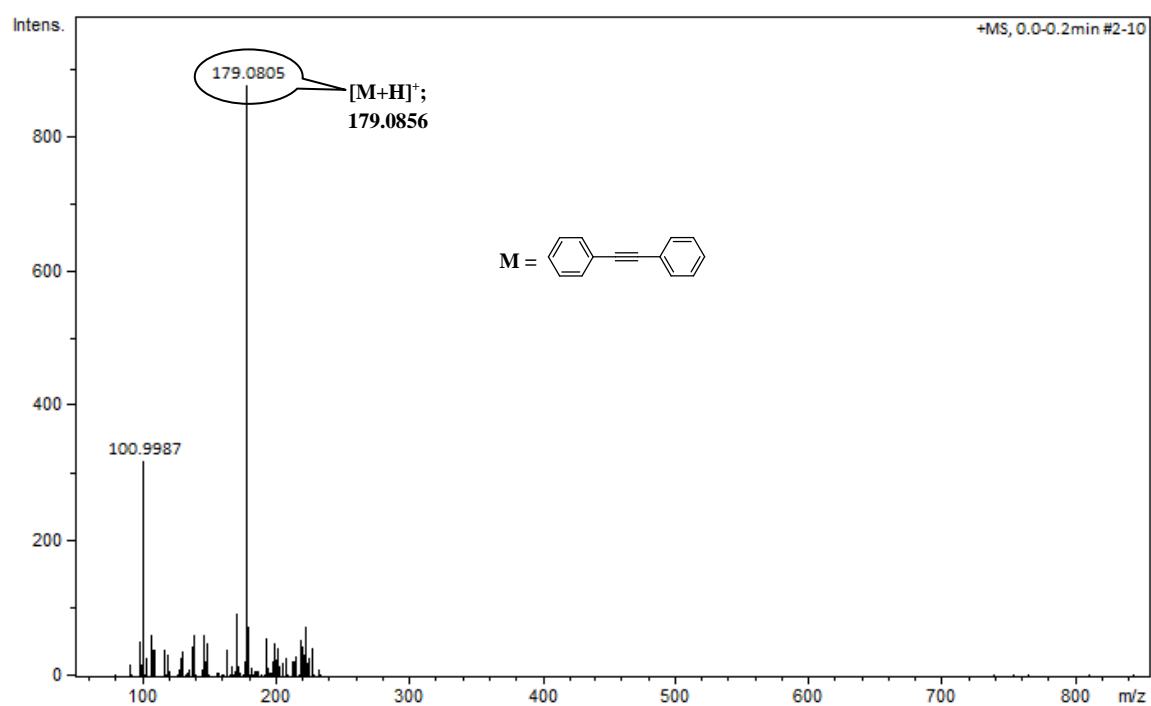


Fig. S24A: ^1H NMR Spectra (CDCl_3 , 500 MHz, ppm) of compound 5b:

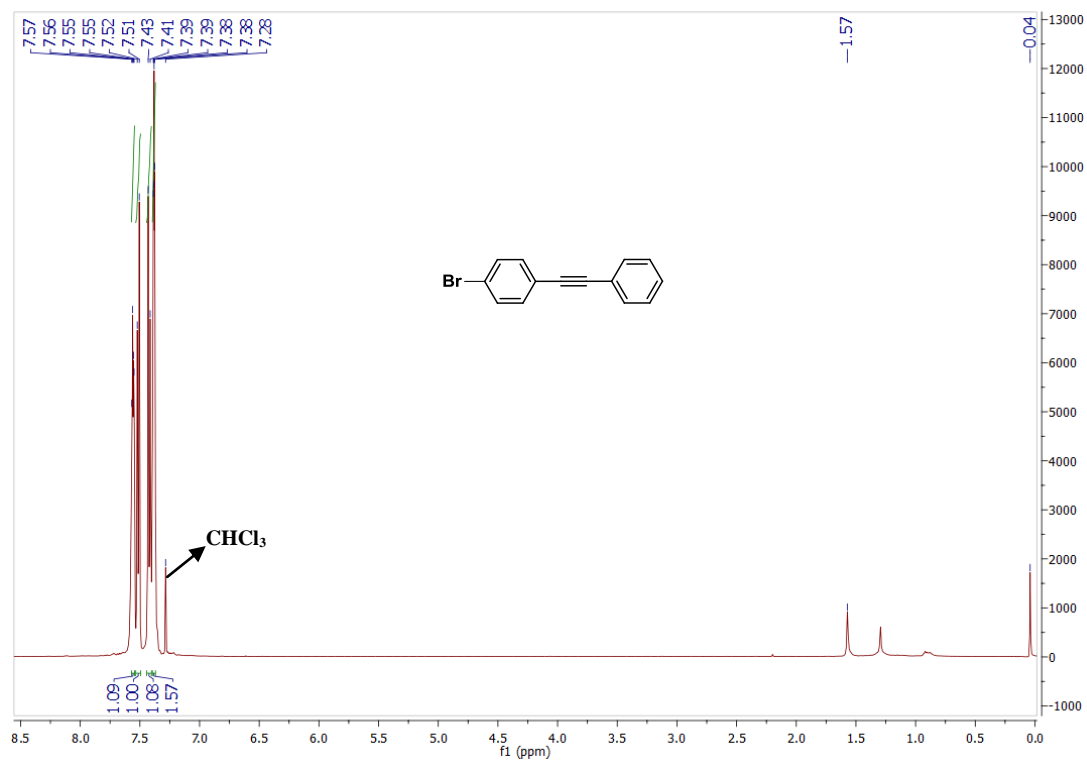


Fig. S24B: ^{13}C NMR Spectra (CDCl_3 , 500 MHz, ppm) of compound 5b:

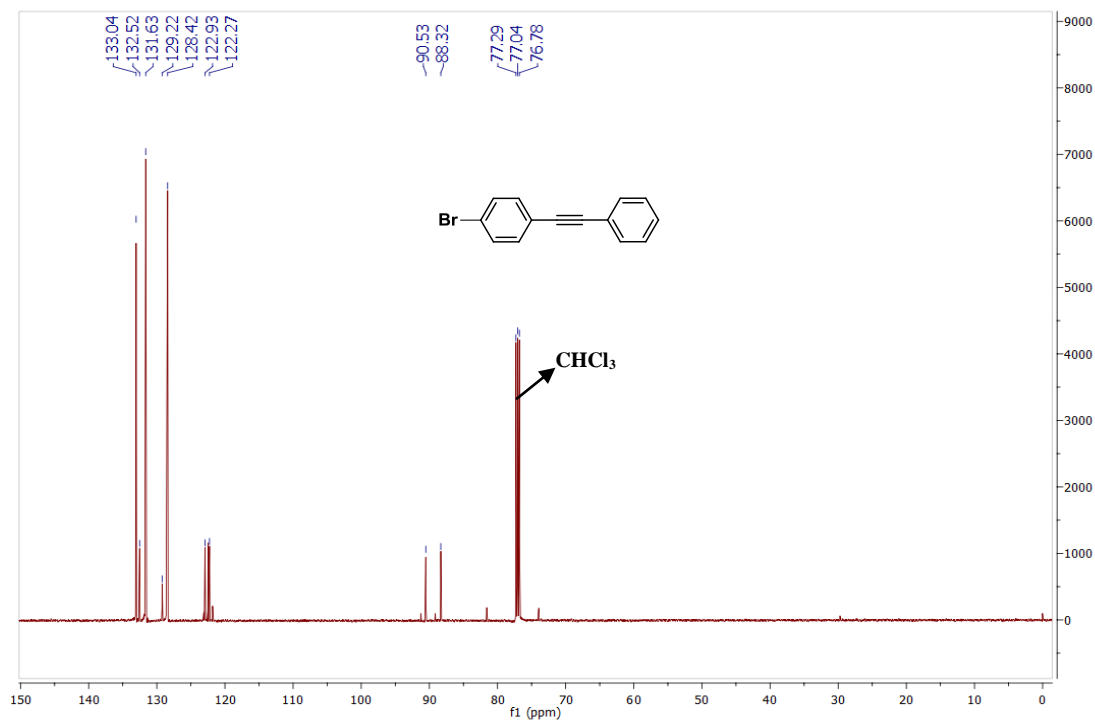


Fig. S25: ESI-MS Spectrum of compound 5b:

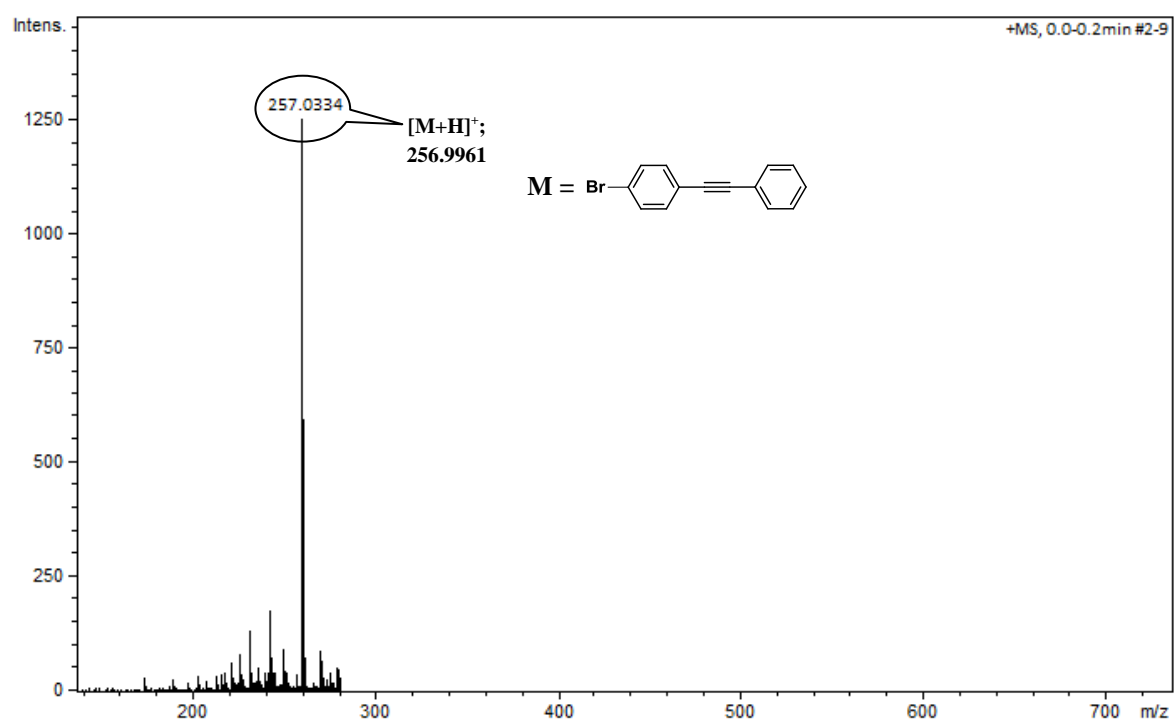


Fig. S26A: ^1H NMR Spectra (DMSO- d_6 , 400 MHz, ppm) of compound 3:

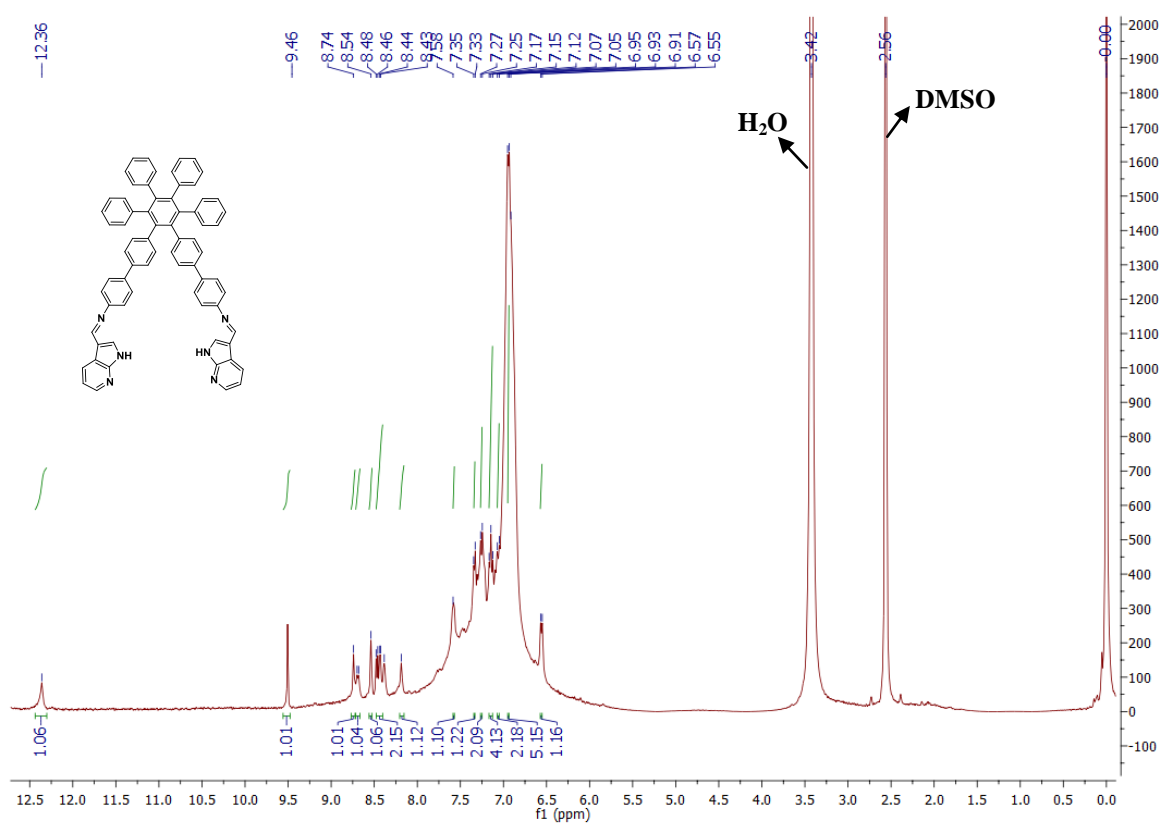


Fig. S26B: Expanded ^1H NMR Spectra (DMSO- d_6 , 400 MHz, ppm) of compound 3:

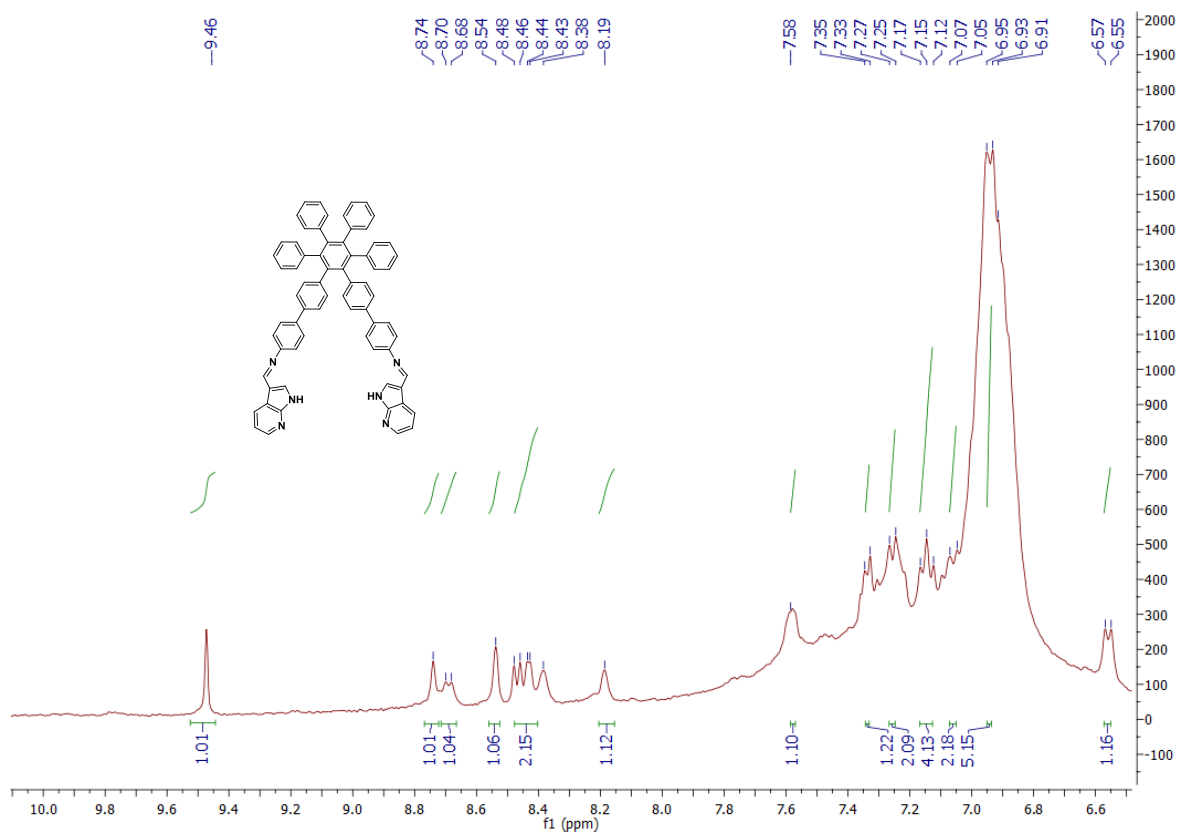


Fig. S27: ^{13}C NMR Spectra (CDCl_3 , 400 MHz, ppm) of compound 3:

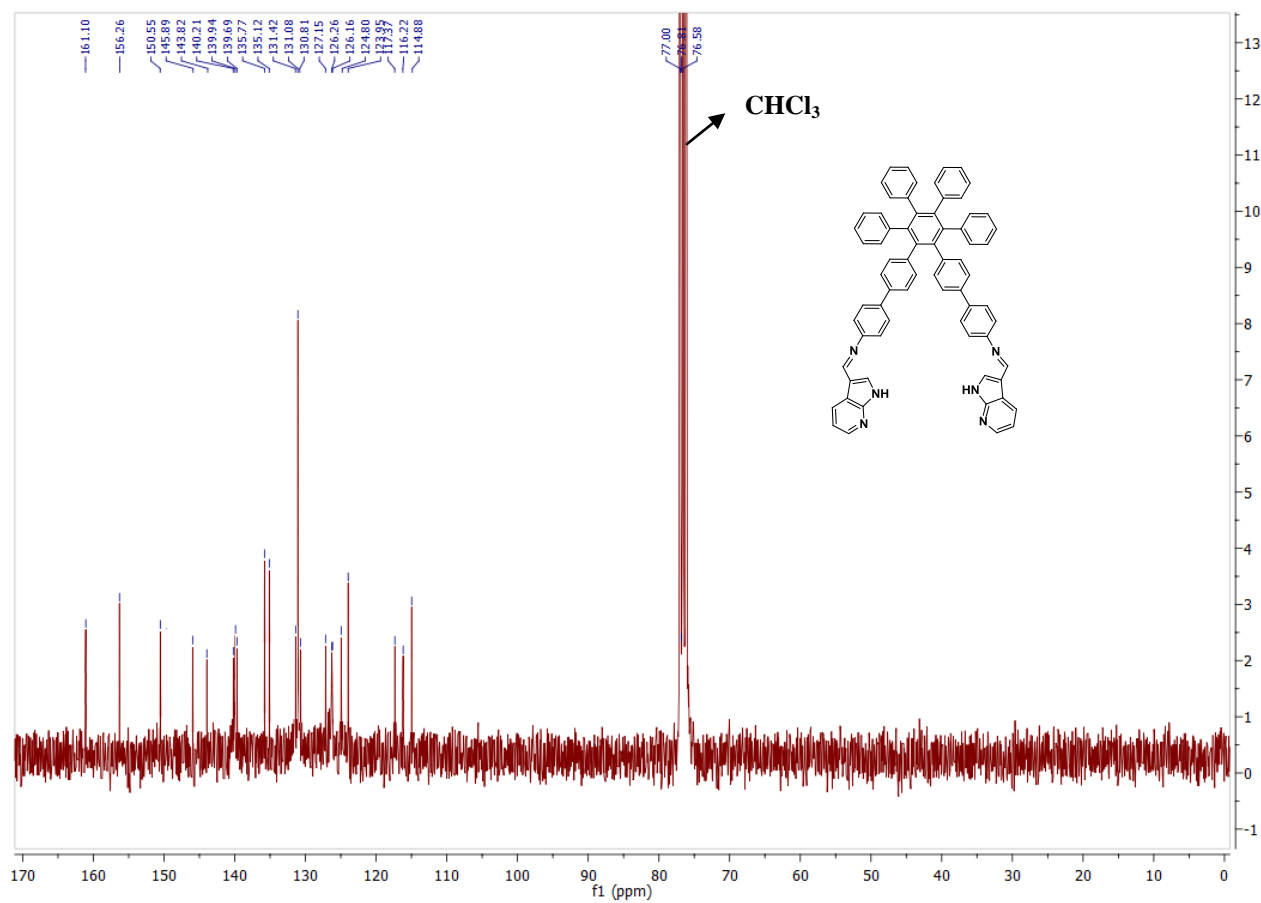


Fig. S28: ESI-MS Spectrum of compound 3:

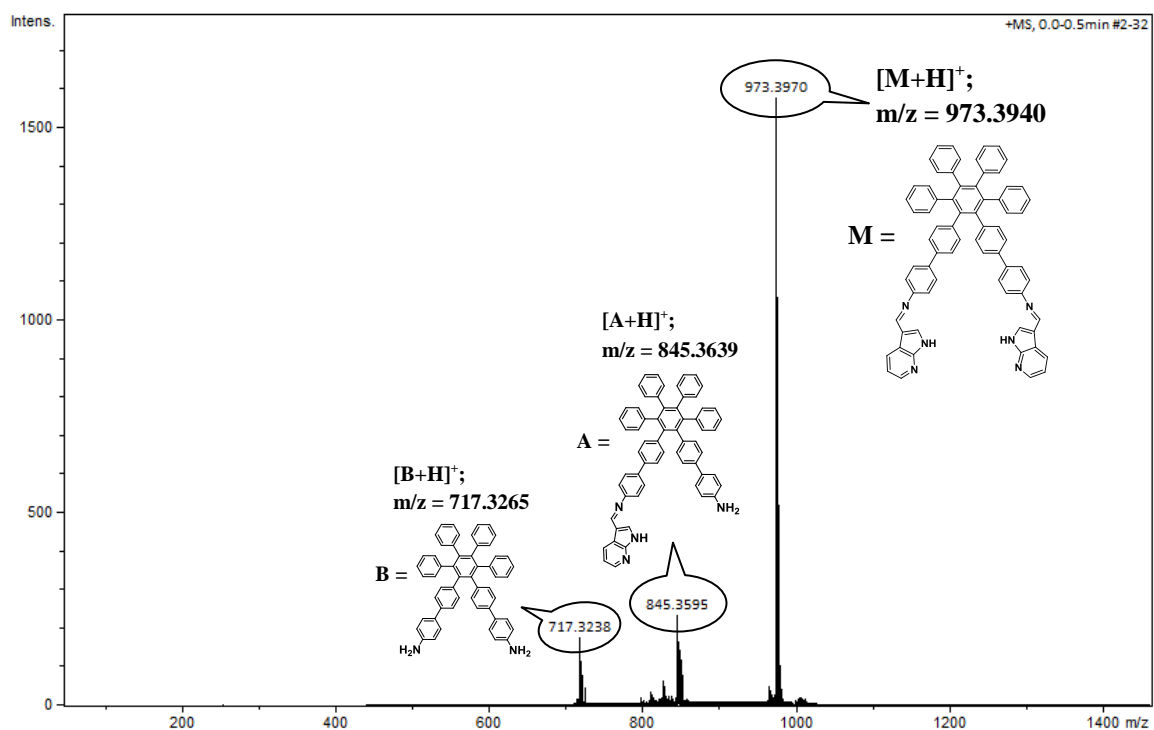


Fig. S29: FT-IR Spectrum of compound 3:

